

1 **Multi-type Galton-Watson processes with**  
2 **affinity-dependent selection applied to antibody**  
3 **affinity maturation**

4 Irene Balelli · Vuk Milišić · Gilles Wainrib

5  
6 Received: date / Accepted: date

7 **Abstract** We analyze the interactions between division, mutation and selec-  
8 tion in a simplified evolutionary model, assuming that the population observed  
9 can be classified into fitness levels. The construction of our mathematical  
10 framework is motivated by the modeling of antibody affinity maturation of  
11 B-cells in Germinal Centers during an immune response. This is a key pro-  
12 cess in adaptive immunity leading to the production of high affinity antibodies  
13 against a presented antigen. Our aim is to understand how the different biolog-  
14 ical parameters affect the system’s functionality. We identify the existence of  
15 an optimal value of the selection rate, able to maximize the number of selected  
16 B-cells for a given generation.

17 **Keywords** Multi-type Galton-Watson process · Germinal center reaction ·  
18 Affinity-dependent selection · Evolutionary landscapes

19 **Mathematics Subject Classification (2010)** 60J85 · 60J80 · 92B99 ·  
20 92D15

21 **Contents**

22 **1 Introduction** . . . . . 2

I. Balelli · V. Milišić  
Université Paris 13, Sorbonne Paris Cité, LAGA, CNRS (UMR 7539), laboratoire  
d’excellence Inflammex. F-93430 - Villetaneuse - France.  
E-mail: balelli@math.univ-paris13.fr · milisic@math.univ-paris13.fr

I. Balelli  
ISPED, Centre INSERM U1219, and INRIA - Statistics in System Biology and Translational  
Medicine Team. F-33000 - Bordeaux - France. E-mail: irene.balelli@inserm.fr

G. Wainrib  
Ecole Normale Supérieure, Département d’Informatique.  
45 rue d’Ulm, 75005 - Paris - France. E-mail: gilles.wainrib@ens.fr

G. Wainrib  
Owkin, Inc. E-mail: gilles.wainrib@owkin.com

23	<b>2</b>	<b>Main definitions and modeling assumptions</b>	4
24	<b>3</b>	<b>Results</b>	6
25	<b>4</b>	<b>Extensions of the model</b>	19
26	<b>5</b>	<b>Conclusions and perspectives</b>	28
27	<b>6</b>	<b>Acknowledgements</b>	33
28	<b>A</b>	<b>Few reminders of classical results on GW processes</b>	35
29	<b>B</b>	<b>Proof of Proposition 2</b>	36
30	<b>C</b>	<b>Deriving the extinction probability of the GC from the multi-type GW process (Section 3.2)</b>	38
31			
32	<b>D</b>	<b>Expected size of the GC derived from the multi-type GW process (Section 3.2)</b>	39
33	<b>E</b>	<b>Proof of Proposition 5</b>	40
34	<b>F</b>	<b>Heuristic proof of Proposition 6</b>	42

## 35 1 Introduction

36 Antibody Affinity Maturation (AAM) takes place in Germinal Centers (GCs),  
 37 specialized micro-environments which form in the peripheral lymphoid or-  
 38 gans upon infection or immunization [37, 10]. GCs are seeded by ten to hun-  
 39 dreds distinct B-cells [34], activated after the encounter with an antigen, which  
 40 initially undergo a phase of intense proliferation [10]. Then, AAM is achieved  
 41 thanks to multiple rounds of division, Somatic Hypermutation (SHM) of the B-  
 42 cell receptor proteins, and subsequent selection of B-cells with improved ability  
 43 of antigen-binding [20]. B-cells which successfully complete the GC reaction  
 44 output as memory B-cells or plasma cells [38, 10]. Indirect evidence suggests  
 45 that only B-cells exceeding a certain threshold of antigen-affinity differentiate  
 46 into plasma cells [30]. The efficiency of GCs is assured by the contribution of  
 47 other immune molecules, for instance Follicular Dendritic Cells (FDCs) and  
 48 follicular helper T-cells (Tfh). Nowadays the key dynamics of GCs are well  
 49 characterized [20, 10, 13, 34]. Despite this there are still mechanisms which re-  
 50 main unclear, such as the dynamics of clonal competition of B-cells, hence  
 51 how the selection acts. In recent years a number of mathematical models of  
 52 the GC reaction has appeared to investigate these questions, such as [22, 40],  
 53 where agent-based models are developed and analyzed through extensive nu-  
 54 merical simulations, or [45] where the authors establish a coarse-grained model,  
 55 looking for optimal values of *e.g.* the selection strength and the initial B-cell  
 56 fitness maximizing the affinity improvement.

57  
 58 Our aim in this paper is to contribute to the mathematical foundations  
 59 of adaptive immunity by introducing and studying a simplified evolutionary  
 60 model inspired by AAM, including division, mutation, affinity-dependent selec-  
 61 tion and death. We focus on interactions between these mechanisms, identify  
 62 and analyze the parameters which mostly influence the system functionality,  
 63 through a rigorous mathematical analysis. This research is motivated by im-  
 64 portant biotechnological applications. Indeed, the fundamental understanding  
 65 of the evolutionary mechanisms involved in AAM have been inspiring many  
 66 methods for the synthetic production of specific antibodies for drugs, vac-  
 67 cines or cancer immunotherapy [2, 19, 32]. This production process involves

68 the selection of high affinity peptides and requires smart methods to gener-  
69 ate an appropriate diversity [9]. Beyond biomedical motivations, the study  
70 of this learning process has also given rise in recent years to a new class of  
71 bio-inspired algorithms [7, 27, 35], mainly addressed to solve optimization and  
72 learning problems.

73  
74 We consider a model in which B-cells are classified into  $N + 1$  affinity  
75 classes with respect to a presented antigen,  $N$  being an integer big enough to  
76 opportunely describe the possible fitness levels of a B-cell with respect to a  
77 specific antigen [41, 43]. A B-cell is able to increase its fitness thanks to SHMs  
78 of its receptors: only about 20% of all mutations are estimated to be affinity-  
79 affecting mutations [31, 33]. By conveniently defining a transition probability  
80 matrix, we can characterize the probability that a B-cell belonging to a given  
81 affinity class passes to another one by mutating its receptors thanks to SHMs.  
82 Therefore we define a selection mechanism which acts on B-cells differently de-  
83 pending on their fitness. We mainly focus on a model of *positive and negative*  
84 *selection* in which B-cells submitted to selection either die or exit the GC as  
85 output cells, according to the strength of their affinity with the antigen. Hence,  
86 in this case, no recycling mechanism is taken into account. Nevertheless the  
87 framework we set is very easy to manipulate: we can define and study other  
88 kinds of affinity-dependent selection mechanisms, and eventually include recy-  
89 cling mechanisms, which have been demonstrated to play an important role in  
90 AAM [39]. We demonstrate that independently from the transition probability  
91 matrix defining the mutational mechanism and the affinity threshold chosen  
92 for positive selection, the optimal selection rate maximizing the number of  
93 output cells for the  $t^{\text{th}}$  generation is  $1/t$ ,  $t \in \mathbb{N}$  (Proposition 6).

94  
95 From a mathematical point of view, we study a class of multi-types Galton-  
96 Watson (GW) processes (*e.g.* [14, 3]) in which, by considering dead and sel-  
97 ected B-cells as two distinct types, we are able to formalize the evolution of  
98 a population submitted to an affinity-dependent selection mechanism. To our  
99 knowledge, the problem of affinity-dependent selection in GW processes has  
100 not been deeply investigated so far.

101  
102 In Section 2 we define the main model analyzed in this paper. We give  
103 as well some definitions that we will use in next sections. Section 3 contains  
104 the main mathematical results. A convenient use of a multi-type GW process  
105 allows to study the evolution of both GC and output cells over time. We de-  
106 termine the optimal value of the selection rate which maximizes the expected  
107 number of selected B-cells at any given maturation cycle in Section 3.3. We  
108 conclude Section 3 with some numerical simulations. In Section 4 we define two  
109 possible variants of the model described in previous sections, and provide some  
110 mathematical results and numerical simulations as well. This evidences how  
111 the mathematical tools used in Section 3 easily apply to define other affinity-  
112 dependent selection models. Finally, in Section 5 we discuss our modeling  
113 assumptions and give possible extensions and limitations of our mathematical

114 model. In order to facilitate the reading of the paper, some technical mathe-  
 115 matical demonstrations, as well as some classical results about Galton-Watson  
 116 theory are reported in the Appendix for interested readers.  
 117

## 118 2 Main definitions and modeling assumptions

119 This section provides the mathematical framework of this article. Let us sup-  
 120 pose that given an antigen target cell  $\bar{\mathbf{x}}$ , all B-cell traits can be divided in  
 121 exactly  $N + 1$  distinct affinity classes, named 0 to  $N$ .

122 **Definition 1** Let  $\bar{\mathbf{x}}$  be the antigen target trait. Given a B-cell trait  $\mathbf{x}$ , we  
 123 denote by  $a_{\bar{\mathbf{x}}}(\mathbf{x})$  the affinity class it belongs to with respect to  $\bar{\mathbf{x}}$ ,  $a_{\bar{\mathbf{x}}}(\mathbf{x}) \in$   
 124  $\{0, \dots, N\}$ . The maximal affinity corresponds to the first class, 0, and the  
 125 minimal one to  $N$ .

**Definition 2** Let  $\mathbf{x}$  be a B-cell trait belonging to the affinity class  $a_{\bar{\mathbf{x}}}(\mathbf{x})$  with  
 respect to  $\bar{\mathbf{x}}$ . We say that its affinity with  $\bar{\mathbf{x}}$  is given by:

$$\text{aff}(\mathbf{x}, \bar{\mathbf{x}}) = N - a_{\bar{\mathbf{x}}}(\mathbf{x})$$

126 Of course, this is not the only possible choice of affinity. Typically affinity  
 127 is represented as a Gaussian function [40, 22], having as argument the distance  
 128 between the B-cell trait and the antigen in the shape space of possible traits.  
 129 In our model this distance corresponds to the index of the affinity class the  
 130 B-cell belongs to (0 being the minimal distance,  $N$  the maximal one). Never-  
 131 theless the choice of the affinity function does not affect our model.  
 132

133 During the GC reaction B-cells are submitted to random mutations. This  
 134 implies switches from one affinity class to another with a given probability.  
 135 Setting these probability means defining a mutational rule on the state space  
 136  $\{0, \dots, N\}$  of affinity classes indices (the formal mathematical definition will  
 137 be given in Section 3.2).  
 138

139 The main model we study in this paper is represented schematically in  
 140 Figure 1. It is defined as follows:

**Definition 3** The process starts with  $z_0 \geq 1$  B-cells entering the GC, belong-  
 ing to some affinity classes in  $\{0, \dots, N\}$ . In case they are all identical, we  
 denote by  $a_0$  the affinity class they belong to, with respect to the antigen tar-  
 get cell  $\bar{\mathbf{x}}$ . At each time step, each GC B-cell can eventually undertake three  
 distinct processes: division, mutation and selection. First of all, each GC B-  
 cell can die with a given rate  $r_d \in [0, 1]$ . If not, each B-cell can divide with  
 rate  $r_{div} \in [0, 1]$ : each daughter cell may have a mutated trait, according to  
 the mutational rule allowed. Hence it eventually belongs to a different affinity  
 class than its mother cell. Clearly, it also happens that a B-cell stays in the  
 GC without dying nor dividing. Finally, with rate  $r_s \in [0, 1]$  each B-cell can

be submitted to selection, which is made according to its affinity with  $\bar{\mathbf{x}}$ . A threshold  $\bar{a}_s$  is fixed: if the B-cell belongs to an affinity class with index greater than  $\bar{a}_s$ , the B-cell dies. Otherwise, the B-cell exits the GC pool and reaches the selected pool. Therefore, for any GC B-cell and at any generation, we have:

$$\begin{cases} \text{Probability of cellular apoptosis: } \mathbb{P}(\text{death}) = r_d \\ \text{Probability of cellular division: } \mathbb{P}(\text{division}) = r_{div} \\ \text{Probability of selection challenge: } \mathbb{P}(\text{selection}) = r_s \end{cases}$$

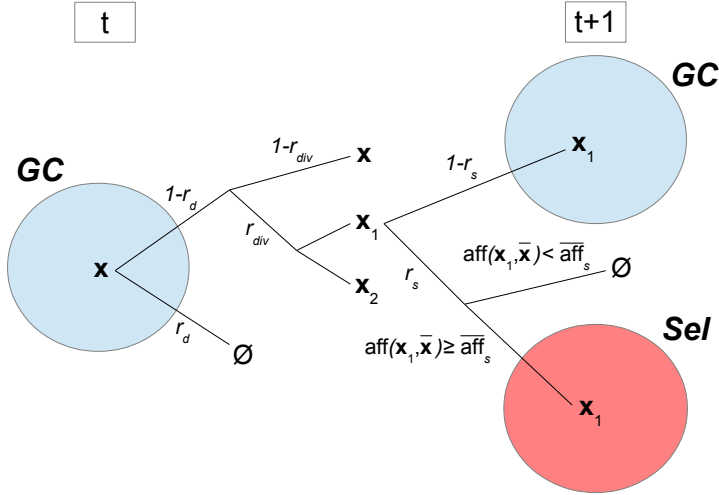


**Figure 1:** Schematic representation of model described by Definition 3. Here we denote by  $\bar{\text{aff}}_s := N - \bar{a}_s$ , the fitness of each B-cell in the affinity class whose index is  $\bar{a}_s$  (see Definitions 1 and 2).

141 Once the GC reaction is fully established ( $\sim$  day 7 after immunization), it  
 142 is polarized into two compartments, named Dark Zone (DZ) and Light Zone  
 143 (LZ) respectively. The DZ is characterized by densely packed dividing B-cells,  
 144 while the LZ is less densely populated and contains FDCs and Tfh cells. The  
 145 LZ is the preferential zone for selection [10]. The transition of B-cells from the  
 146 DZ to the LZ seems to be determined by a timed cellular program: over a 6  
 147 hours period about 50% of DZ B-cells transit to the LZ, where they compete  
 148 for positive selection signaling [6, 36].

149  
 150 Through the entire paper one should keep in mind the following main  
 151 modeling assumptions:

152 *Modeling assumption 1* In our simplified mathematical model we do not take  
 153 into account any spatial factor and in a single time step a GC B-cell can  
 154 eventually undergo both division (with mutation) and selection. Hence the  
 155 time unit has to be chosen big enough to take into account both mechanisms.

156 *Modeling assumption 2* In this paper we are considering discrete-time models.  
 157 The symbol  $t$  always denote a discrete time step, hence it is an integral value.  
 158 We will refer to  $t$  as time, generation, or even maturation cycle to further  
 159 stress the fact that in a single time interval  $[t, t + 1]$  each B-cell within the GC  
 160 population is allowed to perform a complete cycle of division, mutation and  
 161 selection.

162 *Modeling assumption 3* Throughout the entire paper, when we talk about  
 163 death rate (respectively division rate or selection rate) we are referring to  
 164 the probability that each cell has of dying (respectively dividing or being sub-  
 165 mitted to selection) in a single time step.

166

### 167 3 Results

168 In this Section we formalize mathematically the model introduced above. This  
 169 enables the estimation of various qualitative and quantitative measures of the  
 170 GC evolution and of the selected pool as well. In Section 3.1 we show that a  
 171 simple GW process describes the evolution of the size of the GC and determine  
 172 a condition for its extinction. In order to do so, we do not need to know the  
 173 mutational model. Nevertheless, if we want to understand deeply the whole  
 174 reaction we need to consider a  $(N + 3)$ -type GW process, which we introduce  
 175 in Section 3.2. Therefore we determine explicitly other quantities, such as the  
 176 average affinity in the GC and the selected pool, or the evolution of the size  
 177 of the latter. We conclude this section by numerical simulations (Section 3.4).

#### 178 3.1 Evolution of the GC size

179 The aim of this section is to estimate the evolution of the GC size and its  
 180 extinction probability. In order to do so we define a simple GW process, with  
 181 respect to parameters  $r_d, r_{div}$  and  $r_s$ . Indeed, each B-cell submitted to selection  
 182 exits the GC pool, independently from its affinity with  $\bar{x}$ . Hence we apply some  
 183 classical results about generating functions and GW processes ([14], Chapter  
 184 I), which we recall in Appendix A. Proposition 1 gives explicitly the expected  
 185 size of the GC at time  $t$  and conditions for the extinction of the GC.

186 **Definition 4** Let  $Z_t^{(z_0)}, t \geq 0$  be the random variable (rv) describing the GC-  
 187 population size at time  $t$ , starting from  $z_0 \geq 1$  initial B-cells.  $(Z_t^{(z_0)})_{t \in \mathbb{N}}$  is a  
 188 Markov Chain (MC) - since each cell behaves independently from the others  
 189 and from previous generations - on  $\{0, 1, 2, \dots\}$ .

190 If  $z_0 = 1$  and there is no confusion, we denote  $Z_t := Z_t^{(1)}$ . By Definition  
 191 4,  $Z_1$  corresponds to the number of cells in the GC at the first generation,  
 192 starting from a single seed cell. Thanks to Definition 3 one can claim that  
 193  $Z_1 \in \{0, 1, 2\}$ , with the following probabilities:

$$\begin{cases} p_0 := \mathbb{P}(Z_1 = 0) = r_d + (1 - r_d)r_s(1 - r_{div} + r_{div}r_s) \\ p_1 := \mathbb{P}(Z_1 = 1) = (1 - r_d)(1 - r_s)(1 - r_{div} + 2r_{div}r_s) \\ p_2 := \mathbb{P}(Z_1 = 2) = r_{div}(1 - r_d)(1 - r_s)^2 \end{cases} \quad (1)$$

194 As far as next generations are concerned, conditioning to  $Z_t = k$ , *i.e.* at  
 195 generation  $t$  there are  $k$  B-cells in the GC,  $Z_{t+1}$  is distributed as the sum of  
 196  $k$  independent copies of  $Z_1$ :  $\mathbb{P}(Z_{t+1} = k' | Z_t = k) = \mathbb{P}\left(\sum_{i=1}^k Z_1 = k'\right)$ .

197  
 198 Equalities in (1) are derived by identifying the events leading to 0, 1 or  
 199 2 offspring in the GC coming from a single clone. Since these events are in-  
 200 dependent and disjoint, the result follows. For instance there will be 0 new  
 201 individuals in the GC if either the mother cell dies, or it does not die, does  
 202 not divide and is submitted to selection, or it does not die, it does divide and  
 203 both daughter cells are submitted to selection :

$$\begin{aligned} \mathbb{P}(Z_1 = 0) &= \mathbb{P}\left(\text{death} \cup (\text{death}^C \cap \text{division}^C \cap \text{selection}) \cup (\text{death}^C \cap \text{division} \cap \text{selection} \cap \text{selection})\right) \\ &= \mathbb{P}(\text{death}) + \mathbb{P}(\text{death}^C)\mathbb{P}(\text{division}^C)\mathbb{P}(\text{selection}) + \mathbb{P}(\text{death}^C)\mathbb{P}(\text{division})\mathbb{P}(\text{selection})^2 \\ &= r_d + (1 - r_d)(1 - r_{div})r_s + (1 - r_d)r_{div}r_s^2 \end{aligned}$$

204 We have denoted by  $A^C$  the complement of event  $A$ . Expressions for  $p_1$  and  
 205  $p_2$  are obtained proceeding as before.

**Definition 5** Let  $X$  be an integer valued rv,  $p_k := \mathbb{P}(X = k)$  for all  $k \geq 0$ . Its probability generating function (pgf) is given by:

$$F_X(s) = \sum_{k=0}^{+\infty} p_k s^k$$

206 The pgf for  $Z_1$ :

$$\begin{aligned} F(s) &= p_0 + p_1 s + p_2 s^2 \\ &= r_d + (1 - r_d)r_s(1 - r_{div} + r_{div}r_s) \\ &\quad + (1 - r_d)(1 - r_s)(1 - r_{div} + 2r_{div}r_s)s + r_{div}(1 - r_d)(1 - r_s)^2 s^2 \end{aligned} \quad (2)$$

207 By using classical results on Galton-Watson processes (see Appendix A),  
 208 one can prove:

209 **Proposition 1**

210 (i) *The expected size of the GC at time  $t$  and starting from  $z_0$  initial B-cells*  
 211 *is given by:*

$$\mathbb{E}(Z_t^{(z_0)}) = z_0 ((1 - r_d)(1 + r_{div})(1 - r_s))^t \quad (3)$$

212 (ii) Denoted by  $\eta_{z_0}$  the extinction probability of the GC population starting  
 213 from  $z_0$  initial B-cells, one has:

214 – if  $\mathbb{E}(Z_1^{(1)}) \leq 1 \Leftrightarrow r_s \geq 1 - \frac{1}{(1-r_d)(1+r_{div})}$ , then  $\eta_{z_0} = 1$ : the process is  
 215 subcritical

216 – otherwise  $\eta_{z_0} = \eta^{z_0} < 1$ ,  $\eta$  being the smallest fixed point of (2): the  
 217 process is supercritical

218 In particular, the initial number of seed cells  $z_0$  does not affect the crit-  
 219 icality of the process. Nevertheless, in the supercritical case, increasing the  
 220 number of seed B-cells at the beginning of the process makes the probabili-  
 221 ty of extinction decrease. More precisely, in the case  $\eta < 1$ , then  $\eta_{z_0} \rightarrow 0$  if  
 222  $z_0 \rightarrow \infty$ , but we recall that GCs seem to be typically seeded by few B-cells,  
 223 varying from ten to hundreds [34].

224

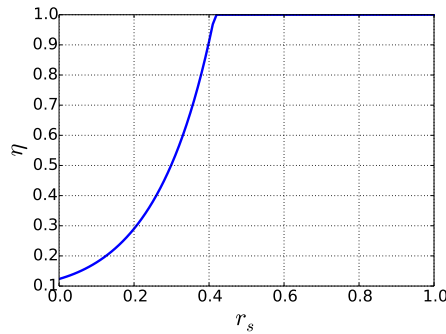


**Figure 2:** Numerical estimation of the extinction probability  $\eta$  of the GC with respect to  $r_s$  for  $r_d = 0.1$  and  $r_{div} = 0.9$ .

225 This section shows that a classical use of a simple GW process enables  
 226 to understand quantitatively the GC growth. Moreover, Proposition 1 (ii)  
 227 gives a condition on the main parameters for the extinction of the GC: if  
 228 the selection pressure is too high, with probability 1 the GC size goes to 0,  
 229 independently from the initial number of seed cells. Intuitively, a too high  
 230 selection pressure prevents those B-cells with bad affinity to improve their  
 231 fitness undergoing further rounds of mutation and division. Most B-cells will  
 232 be rapidly submitted to selection, hence either exit the GC as output cells or  
 233 die by apoptosis if they fail to receive positive selection signals [20]. In Figure  
 234 2 we plot the extinction probability of a GC initiated from a single seed cell  
 235 as a function of  $r_s$  ( $r_d$  and  $r_{div}$  are fixed), in order to stress the presence of  
 236 a threshold effect of the selection probability over the extinction probability.  
 237 The extinction probability of the GC process can give us some further insights  
 238 on factors which are potentially involved in determining the success or failure  
 239 of a GC reaction. This simplified mathematical model suggests that if the

240 selection pressure is too high compared to the division rate (*c.f.* due to Tfh  
 241 signals in the LZ), the GC will collapse with probability 1, preventing the  
 242 generation of high affinity antibodies against the presented antigen, hence an  
 243 efficient immune response.

### 244 3.2 Evolution of the size and fitness of GC and selected pools

245 The GW process defined in the previous Section only describes the size of  
 246 the GC. Indeed, we are not able to say anything about the average fitness of  
 247 GC clones, or the expected number of selected B-cells, or their average affini-  
 248 ty. Hence, we need to consider a more complex model and take into account  
 249 the threshold for positive selection  $\bar{a}_s$ , and the transition probability matrix  
 250 characterizing the mutational rule. Indeed, the mutational process is described  
 251 as a Random Walk (RW) on the state space  $\{0, \dots, N\}$  of affinity classes in-  
 252 dices. The mutational rule reflects the edge set associated to the state-space  
 253  $\{0, \dots, N\}$ : this is given by a transition probability matrix.

**Definition 6** Let  $(\mathbf{X}_t)_{t \geq 0}$  be a RW on the state-space of B-cell traits descri-  
 bing a pure mutational process of a B-cell during the GC reaction. We denote  
 by  $\mathcal{Q}_N = (q_{ij})_{0 \leq i, j \leq N}$  the transition probability matrix over  $\{0, \dots, N\}$  which  
 gives the probability of passing from an affinity class to another during the  
 given mutational model. For all  $0 \leq i, j \leq N$ :

$$q_{ij} = \mathbb{P}(a_{\bar{x}}(\mathbf{X}_{t+1}) = j \mid a_{\bar{x}}(\mathbf{X}_t) = i)$$

254 From a biological point of view, these probabilities could be obtained *e.g.* by  
 255 identifying which key mutations are the most relevant in determining changes  
 256 in the fitness of a clone to a specific antigen and at which frequency they are  
 257 produced.

258 We introduce a multi-type GW Process (see for instance [3], chapter V).

260 **Definition 7** Let  $\mathbf{Z}_t^{(i)} = (Z_{t,0}^{(i)}, \dots, Z_{t,N+2}^{(i)})$ ,  $t \geq 0$  be a MC where for all  $0 \leq$   
 261  $j \leq N$ ,  $Z_{t,j}^{(i)}$  describes the number of GC B-cells belonging to the  $j^{\text{th}}$ -affinity  
 262 class with respect to  $\bar{x}$ ,  $Z_{t,N+1}^{(i)}$  the number of selected B-cells and  $Z_{t,N+2}^{(i)}$  the  
 263 number of dead B-cells at generation  $t$ , when the process is initiated in state  
 264  $\mathbf{i} = (i_0, \dots, i_N, 0, 0)$ .

265 Let  $m_{ij} := \mathbb{E}[Z_{1,j}^{(i)}]$  the expected number of offspring of type  $j$  of a cell of  
 266 type  $i$  in one generation. We collect all  $m_{ij}$  in a matrix,  $\mathcal{M} = (m_{ij})_{0 \leq i, j \leq N+2}$ .  
 267 We have:

$$\mathbb{E}[\mathbf{Z}_t^{(i)}] = \mathbf{i} \mathcal{M}^t \quad (4)$$

268 Supposing matrix  $\mathcal{Q}_N$  given (Definition 6), describing the probability to  
 269 switch from one affinity class to another thanks to a single mutation event,  
 270 one can explicitly derive the elements of  $\mathcal{M}$ .

**Proposition 2**  $\mathcal{M}$  is a  $(N+3) \times (N+3)$  matrix defined as a block matrix:

$$\mathcal{M} = \begin{pmatrix} \mathcal{M}_1 & \mathcal{M}_2 \\ \mathbf{0}_{2 \times (N+1)} & \mathcal{I}_2 \end{pmatrix}$$

271 Where:

- 272 –  $\mathbf{0}_{2 \times (N+1)}$  is a  $2 \times (N+1)$  matrix with all entries 0;  
 273 –  $\mathcal{I}_n$  is the identity matrix of size  $n$ ;  
 274 –  $\mathcal{M}_1 = 2(1-r_d)r_{div}(1-r_s)\mathcal{Q}_N + (1-r_d)(1-r_{div})(1-r_s)\mathcal{I}_{N+1}$   
 275 –  $\mathcal{M}_2 = (m_{2,ij})$  is a  $(N+1) \times 2$  matrix where for all  $i \in \{0, \dots, N\}$ :  
 276 – if  $i \leq \bar{a}_s$ :

$$277 \quad m_{2,i1} = (1-r_d)(1-r_{div})r_s + 2(1-r_d)r_{div}r_s \sum_{j=0}^{\bar{a}_s} q_{ij},$$

$$278 \quad m_{2,i2} = r_d + 2(1-r_d)r_{div}r_s \sum_{j=\bar{a}_s+1}^N q_{ij}$$

- 279 – if  $i > \bar{a}_s$ :

$$280 \quad m_{2,i1} = 2(1-r_d)r_{div}r_s \sum_{j=0}^{\bar{a}_s} q_{ij},$$

$$281 \quad m_{2,i2} = r_d + (1-r_d)(1-r_{div})r_s + 2(1-r_d)r_{div}r_s \sum_{j=\bar{a}_s+1}^N q_{ij}$$

282 The proof of Proposition 2 is available in Appendix B. It is based on the  
 283 computation of the probability generating function of  $\mathbf{Z}_1$ .

284 *Remark 1* Independently from the given mutational model, the expected number  
 285 of selected or dead B-cells that each GC B-cell can produce in a single time  
 286 step is given by  $\alpha := r_d + (1-r_d)(1+r_{div})r_s$ . All rows of  $\mathcal{M}_2$  sum to  $\alpha$  in-  
 287 dependently from the probability that each clone submitted to selection has  
 288 of being positive selected, which we recall is 1 if it belongs to the  $i^{\text{th}}$  affinity  
 289 class,  $i \leq \bar{a}_s$ , zero otherwise.

290 Of course in the multi-type context we recover again results from Section  
 291 3.1, such as the extinction probability of the GC (detailed in Appendix C).

292

293 In order to determine the expected number of selected cells at a given time  
 294  $t$ , we need to introduce another multi-type GW process.

295 **Definition 8** Let  $\tilde{\mathbf{z}}_t^{(i)} = (\tilde{z}_{t,0}^{(i)}, \dots, \tilde{z}_{t,N+2}^{(i)})$ ,  $t \geq 0$  be a MC where for all  $0 \leq$   
 296  $j \leq N$ ,  $\tilde{z}_{t,j}^{(i)}$  describes the number of GC B-cells belonging to the  $j^{\text{th}}$ -affinity  
 297 class with respect to  $\bar{\mathbf{x}}$ ,  $\tilde{z}_{t,N+1}^{(i)}$  the number of selected B-cells and  $\tilde{z}_{t,N+2}^{(i)}$  the  
 298 number of dead B-cells at generation  $t$ , when the process is initiated in state  
 299  $\mathbf{i} = (i_0, \dots, i_N, 0, 0)$  and before the selection mechanism is performed for the  
 300  $t^{\text{th}}$ -generation.

301 Proceeding as we did for  $\mathbf{Z}_t^{(i)}$ , we can determine a matrix  $\widetilde{\mathcal{M}}$  whose elements  
 302 are  $\widetilde{m}_{ij} := \mathbb{E}[\widetilde{Z}_{1,j}^{(i)}]$  for all  $i, j \in \{0, \dots, N+2\}$ .

**Proposition 3**  $\widetilde{\mathcal{M}}$  is a  $(N+3) \times (N+3)$  matrix, which only depends on matrix  $\mathcal{Q}_N$ ,  $r_d$  and  $r_{div}$  and can be defined as a block matrix as follows:

$$\widetilde{\mathcal{M}} = \begin{pmatrix} \widetilde{\mathcal{M}}_1 & \widetilde{\mathcal{M}}_2 \\ \mathbf{0}_{2 \times (N+1)} & \mathcal{I}_2 \end{pmatrix}$$

303 Where:

- 304 –  $\widetilde{\mathcal{M}}_1 = 2(1-r_d)r_{div}\mathcal{Q}_N + (1-r_d)(1-r_{div})\mathcal{I}_{N+1}$
- 305 –  $\widetilde{\mathcal{M}}_2 = (\mathbf{0}_{N+1}, r_d \cdot \mathbf{1}_{N+1})$ , where  $\mathbf{0}_{N+1}$  (resp.  $\mathbf{1}_{N+1}$ ) is a  $(N+1)$ -column  
 306 vector whose elements are all 0 (resp. 1).

307 One could prove that:

$$\mathbb{E}[\widetilde{\mathbf{Z}}_t^{(i)}] = \mathbf{i}\mathcal{M}^{t-1}\widetilde{\mathcal{M}} \quad (5)$$

308 **Proposition 4** Let  $\mathbf{i}$  be the initial state,  $|\mathbf{i}|$  its 1-norm ( $|\mathbf{i}| := \sum_{j=0}^{N+2} \mathbf{i}_j$ ).

- 309 – The expected size of the GC at time  $t$ :

$$\sum_{k=0}^N (\mathbf{i}\mathcal{M}^t)_k \left( = |\mathbf{i}| ((1-r_d)(1+r_{div})(1-r_s))^t \right) \quad (6)$$

- 310 – The average affinity in the GC at time  $t$ :

$$\frac{\sum_{k=0}^N (N-k)(\mathbf{i}\mathcal{M}^t)_k}{\sum_{k=0}^N (\mathbf{i}\mathcal{M}^t)_k} \quad (7)$$

- 311 – Let  $S_t$ ,  $t \geq 1$  denotes the random variable describing the number of selected  
 312 B-cells at time  $t$ . By hypothesis  $S_0 = 0$ .  $(S_t)_{t \in \mathbb{N}}$  is a MC on  $\{0, 1, 2, \dots\}$ .  
 313 The expected number of selected B-cells at time  $t$ ,  $t \geq 1$ :

$$\mathbb{E}(S_t) = r_s \sum_{k=0}^{\bar{a}_s} (\mathbf{i}\mathcal{M}^{t-1}\widetilde{\mathcal{M}})_k \quad (8)$$

- 314 – The expected number of selected B-cells produced until time  $t$ :

$$\mathbb{E} \left[ \sum_{n=0}^t S_n \right] = \mathbb{E} \left[ \left( \mathbf{Z}_t^{(i)} \right)_{N+1} \right] = (\mathbf{i}\mathcal{M}^t)_{N+1} \quad (9)$$

315 – The average affinity of selected B-cells at time  $t$ ,  $t \geq 1$ :

$$\frac{\sum_{k=0}^{\bar{a}_s} (N-k) \left( \mathbf{iM}^{t-1} \widetilde{\mathcal{M}} \right)_k}{\sum_{k=0}^{\bar{a}_s} \left( \mathbf{iM}^{t-1} \widetilde{\mathcal{M}} \right)_k} \quad (10)$$

316 – The average affinity of selected B-cells until time  $t$ :

$$\frac{r_s \sum_{n=1}^t \sum_{k=0}^{\bar{a}_s} (N-k) \left( \mathbf{iM}^{n-1} \widetilde{\mathcal{M}} \right)_k}{\left( \mathbf{iM}^t \right)_{N+1}} \quad (11)$$

317 *Proof* Equations (6) and (9) are a direct application of what stated in Equation  
 318 (17). Indeed, Equation (17) states that  $\mathbf{iM}^t$  contains the expectation of  
 319 the number of all types cells at generation  $t$  when the process is started in  
 320  $\mathbf{i}$ . Hence the expectation of the size of the GC at the  $t^{\text{th}}$  generation is given  
 321 by  $\sum_{k=0}^N (\mathbf{iM}^t)_k$ , since the GC at generation  $t$  contains all alive non-selected  
 322 B-cells, irrespectively from their affinity. Similarly, the expected number of selected  
 323 B-cells until time  $t$  (9) corresponds to the expectation of the  $(N+1)^{\text{th}}$ -  
 324 type cell,  $(\mathbf{iM}^t)_{N+1}$ .

325

The proof of Equation (8) is based on Equation (5), which allows to estimate the number of GC B-cells at generation  $t$  which are susceptible of being challenged by selection. One can remark that the expected number of selected B-cells at time  $t$  is obtained from the expected number of B-cells in GC at time  $t$  (before the selection mechanism is performed) having fitness good enough to be positive selected. This is given by  $\sum_{k=0}^{\bar{a}_s} \left( \mathbf{iM}^{t-1} \widetilde{\mathcal{M}} \right)_k$ , thanks to (5). The result follows by multiplying this expectation by the probability that each of these B-cells is submitted to mutation, *i.e.*  $r_s$ . Finally, results about the average affinity in both the GC and the selected pool (Equations (7), (10) and (11)) are obtained from the previous ones (*c.f.* (6), (8) and (9)) by multiplying the number of individuals belonging to the same class by their fitness (Definition 2), and dividing by the total number of individuals in the considered pool. The definition of affinity as a function of the affinity classes, determines Equations (7), (10) and (11). Indeed, the affinity of the  $k^{\text{th}}$ -affinity class is given by  $N - k$ .  $\square$

326 *Remark 2* The expected size of the GC at time  $t$  can be obtained applying a  
 327 simple GW process (Section 3.1) and is given by (3). It is possible to prove  
 328 the equality in brackets in Equation (6) starting from the  $(N+3)$ -type GW  
 329 process. The interested reader can address to Appendix D for the detailed  
 330 proof.

331 3.3 Optimal value of  $r_s$  maximizing the expected number of selected B-cells  
332 at time  $t$

333 What is the behavior of the expected number of selected B-cells as a function  
334 of the model parameters? In particular, is there an optimal value of the selec-  
335 tion rate which maximizes this number? In this section we show that, indeed,  
336 the answer is positive.

337 To do so we detail hereafter the computation of  $\mathbb{E}(S_t)$  (Equation (8)), given  
338 by Proposition 4.

339 Let us suppose, for the sake of simplicity, that  $\mathcal{Q}_N$  is diagonalizable:

$$340 \quad \mathcal{Q}_N = R\Lambda_N L, \quad (12)$$

342 where  $\Lambda_N = \text{diag}(\lambda_0, \dots, \lambda_N)$ , and  $R = (r_{ij})$  (resp.  $L = (l_{ij})$ ) is the transition  
343 matrix whose rows (resp. lines) contain the right (resp. left) eigenvectors of  
344  $\mathcal{Q}_N$ , corresponding to  $\lambda_0, \dots, \lambda_N$ .

345

**Proposition 5** *Let us suppose that at  $t=0$  there is a single B-cell entering the GC belonging to the  $i^{\text{th}}$ -affinity class with respect to the target cell. Moreover, let us suppose that  $\mathcal{Q}_N = R\Lambda_N L$ . For all  $t \in \mathbb{N}$ , the expected number of selected B-cells at time  $t$ , is:*

$$\mathbb{E}(S_t) = r_s(1-r_s)^{t-1}(1-r_d)^t \sum_{\ell=0}^N (2\lambda_\ell r_{div} + 1 - r_{div})^\ell \sum_{k=0}^{\bar{a}_s} r_{i\ell} l_{\ell k},$$

346 The proof of Proposition 5 is detailed in Appendix E.

347

348 As an immediate consequence of Proposition 5, we can claim:

**Proposition 6** *For all  $t^* \in \mathbb{N}$  fixed, the value  $r_s^* := r_s(t^*)$  which maximizes the expected number of selected B-cells at the  $t^{*\text{th}}$  maturation cycle is:*

$$r_s^* = \frac{1}{t^*}$$

*Proof* Since  $(1-r_d)^t \sum_{\ell=0}^N (2\lambda_\ell r_{div} + 1 - r_{div})^\ell \sum_{k=0}^{\bar{a}_s} r_{i\ell} l_{\ell k}$  is a non negative quantity independent from  $r_s$ , the value of  $r_s$  which maximizes  $\mathbb{E}(S_{t^*})$  is the one that maximizes  $r_s(1-r_s)^{t^*-1}$ . The result trivially follows.  $\square$

349 This result suggests that the selection rate in GCs is tightly related to  
350 the timing of the peak of a GC response, *i.e.* the timing corresponding to the  
351 maximal production of output cells (this timing can be determined *e.g.* by ob-  
352 serving the concentration in blood of produced specific B-cells after infection  
353 or vaccination). In particular, following this model, GCs which peak early (*e.g.*  
354 for whom the maximal output cell production is reached in a few days) are

possibly characterized by a higher selection pressure than GCs peaking later. The peak of a typical GC reaction, measured as the average GC volume, has been estimated to be close to day 12 post immunization or a few days before [42], which is consistent with the observation of plasma cell response peak after immunization, *e.g.* [24]. Moreover, an high selection rate could also prevent a correct and efficient establishment of an immune response (*c.f.* results about extinction probability - Proposition 1). In addition, from a biological viewpoint, a too demanding selection pressure could avoid the generation of advantageous mutations, hence their fixation.

*Remark 3* Under certain hypotheses about the mutational model and the GC evolution, one could justify the claim of Proposition 6 by heuristic arguments, without considering the  $(N+3)$ -type GW process. This leads to approximately estimate the expected number of selected B-cells at time  $t$  (Appendix F). Figure 4 (a) shows the peak of positive selected B-cells at generation  $t$  for a certain set of parameters.

### 3.4 Numerical simulations

We evaluate numerically results of Proposition 4. The  $(N+3)$ -type GW process allows a deeper understanding of the dynamics of both populations: inside the GC and in the selected pool. Through numerical simulations we emphasize the dependence of the quantities defined in Proposition 4 on parameters involved in the model.

In previous works [5, 4] we have modeled B-cells and antigens as  $N$ -length binary strings, hence their traits correspond to elements of  $\{0, 1\}^N$ . In this context we have characterized affinity using the Hamming distance between B-cell and antigen representing strings. The idea of using a  $N$ -dimensional shape space to represent antibodies traits and their affinity with respect to a specific antigen has already been employed (*e.g.* [28, 22, 17]), and  $N$  typically varies from 2 to 4. In the interests of simplification, we chose to set  $N = 2$ . Moreover, from a biological viewpoint, this choice means that we classify the amino-acids composing B-cell receptors strings into 2 classes, which could represent amino-acids negatively and positively charged respectively. Charged and polar amino-acids are the most responsible in creating bonds which determine the antigen-antibody interaction [26].

While performing numerical simulations (Sections 3.4 and 4.2) we refer to the following transition probability matrix on  $\{0, \dots, N\}$ :

**Definition 9** For all  $i, j \in \{0, \dots, N\}$ :

$$q_{ij} = \mathbb{P}(a_{\bar{\mathbf{x}}}(\mathbf{X}_{t+1}) = j \mid a_{\bar{\mathbf{x}}}(\mathbf{X}_t) = i) = \begin{cases} i/N & \text{if } j = i - 1 \\ (N - i)/N & \text{if } j = i + 1 \\ 0 & \text{if } |j - i| \neq 1 \end{cases}$$



Table 1: Parameter choice for simulations in Sections 3.4 (unless stated otherwise).

$N$	$r_s$	$r_d$	$r_{div}$	$a_0$	$\bar{a}_s$
10	0.1	0.1	0.9	3	3

416 We perform numerical simulations to better appreciate how the dynamics  
 417 of the GC and positive selected clones populations are related and evolve  
 418 depending on model parameters. In the case of a subcritical GC, by model  
 419 definition selected clones stabilize at a given level once the GC becomes ex-  
 420 tinct. Hence we conveniently chose a parameter set (Table 1) which implies  
 421 a supercritical GC (Proposition 1): with great probability the simulated GC  
 422 goes through explosion, and so the selected population does.

### 423 3.4.1 Evolution of the GC population

424 The evolution of the size of the GC can be studied by using the simple GW  
 425 process defined in Section 3.1. Equation (3), in the case of a single initial B-cell,  
 426 evidences that the expected number of B-cells within the GC for this model  
 427 only depends on  $r_d$ ,  $r_{div}$  and  $r_s$  and it is not driven by the initial affinity, nor  
 428 by the threshold chosen for positive selection  $\bar{a}_s$ , nor by the mutational rule.

429 Equation (3) evidences that, independently from the transition probabili-  
 430 ty matrix defining the mutational mechanism, the GC size at time  $t$  increases  
 431 with  $r_{div}$  and decreases for increasing  $r_s$  and  $r_d$ . Moreover, the impact of these  
 432 last two parameters is the same for the growth of the GC. One could expect  
 433 this behavior since the effect of both the death and the selection on a B-cell  
 434 is the exit from the GC.  
 435

436 In order to study the evolution of the average affinity within the GC, we  
 437 need to refer to the  $(N + 3)$ -type GW process defined in Section 3.2.  
 438

**Proposition 7** *Let us suppose that  $\mathcal{Q}_N = R\Lambda_N L$ . The average affinity within the GC at time  $t$ , starting from a single B-cell belonging to the  $i^{\text{th}}$ -affinity class with respect to  $\bar{\mathbf{x}}$  is given by:*

$$N - \frac{\sum_{\ell=0}^N (2\lambda_{\ell} r_{div} + 1 - r_{div})^t \sum_{k=0}^N k \cdot r_{i\ell} l_{\ell k}}{(1 + r_{div})^t},$$

*Proof* It follows directly from Equations (7) and by considering the eigende-  
 composition of matrix  $\mathcal{Q}$ . One has to consider the expression of the  $t^{\text{th}}$  power  
 of matrix  $\mathcal{M}$  (which can be obtained recursively, see Appendix E): one can

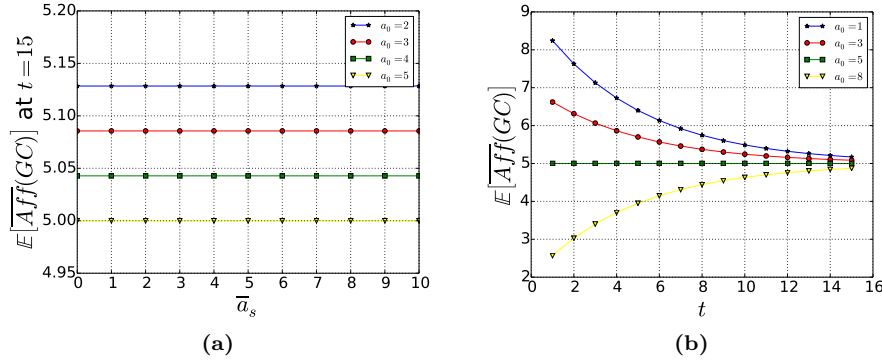


**Figure 3:** (a) Dependence of the expected average affinity in the GC on  $\bar{a}_s$  at time  $t = 15$ , for different values of  $a_0$ . The average affinity in the GC is constant with respect to  $\bar{a}_s$ . (b) The evolution during time of the expected average affinity in the GC for different values of  $a_0$ . The average affinity converges through  $N/2$ , due to the stationary distribution of  $Q_N$ , the binomial probability distribution.

prove that the first  $N + 1$  components of the  $i^{\text{th}}$ -row of matrix  $\mathcal{M}^t$  are the elements of the  $i^{\text{th}}$ -row of matrix  $RD^tL$ , where  $D = 2(1 - r_d)r_{div}(1 - r_s)A_N + (1 - r_d)(1 - r_{div})(1 - r_s)\mathcal{I}_{N+1}$  is a diagonal matrix.  $\square$

439 It is obvious from Proposition 7 that this quantity only depends on the  
 440 initial affinity with the target trait, the transition probability matrix  $Q_N$  and  
 441 the division rate  $r_{div}$ . The average affinity within the GC does not depend on  
 442  $\bar{a}_s$  (as one can clearly see in Figure 3 (a)), nor by  $r_s$  or  $r_d$ . One can intuitively  
 443 understand this behavior: independently from their fitness, all B-cells submitted  
 444 to mutation exit the GC. Moreover,  $r_s$  and  $r_d$  impact the GC size, but  
 445 not its average affinity, as selection and death affect all individuals of the GC  
 446 independently from their fitness.

447  
 448 It can be interesting to observe the evolution of the expected average affinity  
 449 within the GC during time. Numerical simulations of our model show that  
 450 the expected average affinity in the GC converges through  $N/2$ , independently  
 451 from the affinity of the first naive B-cell (Figure 3 (b)). This depends on the  
 452 mutational model we choose for these simulations. Indeed, providing that the  
 453 GC is in a situation of explosion, for  $t$  big enough the distribution of GC clones  
 454 within the affinity classes is governed by the stationary distribution of matrix  
 455  $Q_N$  [4]. Since for  $Q_N$  given by Definition 9 one can prove that the stationary  
 456 distribution over  $\{0, \dots, N\}$  is the binomial probability distribution [5], the  
 457 average affinity within the GC will quickly stabilizes at a value of  $N/2$ . Note  
 458 that for these simulations we chose  $N = 10$ , hence affinities are in the range  
 459  $[0, 10]$ .

460 3.4.2 Evolution of the selected pool

461 The evolution of the number of selected B-cells during time necessarily depends on the evolution of the GC. In particular, let us suppose we are in the  
 462 supercritical case, *i.e.* the extinction probability of the GC is strictly smaller  
 463 than 1. Then, with positive probability, the GC explodes and so does the selected  
 464 pool. On the other hand, if the GC extinguishes, the number of selected  
 465 B-cells will stabilize at a constant value, as once a B-cell is selected it can only  
 466

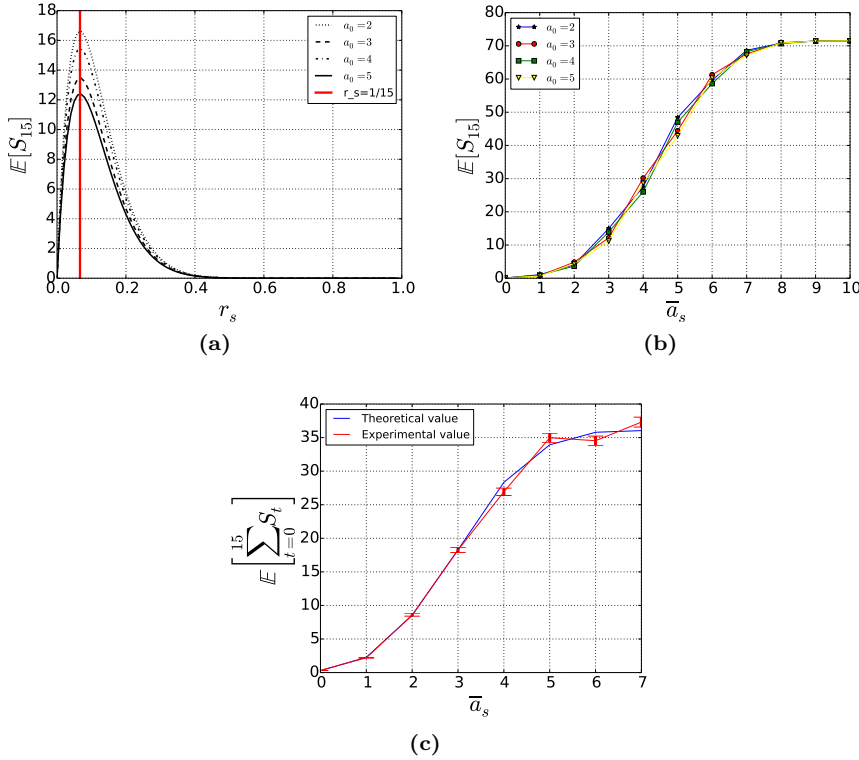


**Figure 4:** (a-b) Expected number of selected B-cells for the time step  $t = 15$  for different values of  $a_0$ , depending on  $r_s$  and  $\bar{a}_s$  respectively. There exists an optimal value of  $r_s$  maximizing the expected number of selected B-cells for a given generation. This value is independent from  $a_0$  and is equal to  $1/t$  as demonstrated in Proposition 6: the red vertical line in (a) corresponds to this value. (c) Comparison between the expected number of selected B-cells until time  $t$  given by evaluation of the theoretical formula (Equation (9)), and the empirical value obtained as the mean over 4000 simulations. Vertical bars denotes the corresponding estimated standard deviations. Here  $N = 7$  and  $r_s = 0.3$ .

467 stay unchanged in the selected pool.

468 As demonstrated in Section 3.3, there exists an optimal value of the pa-  
 469 rameter  $r_s$  which maximizes the expected number of selected B-cells at time  
 470  $t$ . Figure 4 (a) evidences this fact. Moreover, as expected, simulations show  
 471 that the expected size of selected B-cells at a given time  $t$  increases with the  
 472 threshold  $\bar{a}_s$  chosen for positive selection (Figure 4 (b)). This is a consequence  
 473 of Proposition 5:  $\bar{a}_s$  determines the number of elements of the sum  $\sum_{k=0}^{\bar{a}_s} r_{i\ell}l_{\ell k}$ .

474  
 475 Figure 4 (c) underlines the correspondence between theoretical results  
 476 given by Proposition 4 and numerical values obtained by simulating the evo-  
 477 lutionary process described by Definition 3. In particular Figure 4 (c) shows  
 478 the expected (resp. average) number of selected B-cells produced until time  
 479  $t = 15$  depending on the threshold chosen for positive selection,  $\bar{a}_s$ .

481 *Remark 5* We recall that values expressed on y-axes of all graphs in Figure 4  
 482 (and later in Figures 8 to 10) describe the expected number of some groups  
 483 of B-cells (*e.g.* GC B-cells, output B-cells) generated at a given time step or  
 484 after a given number of maturation cycles. Henceforth this is an adimensional  
 485 number. It is of course envisageable to translate these values into concentra-  
 486 tions of some specific B-cell phenotypes into *e.g.* blood or tissue samples in  
 487 order to interpret theoretical results and compare them to biological data.

## 488 4 Extensions of the model

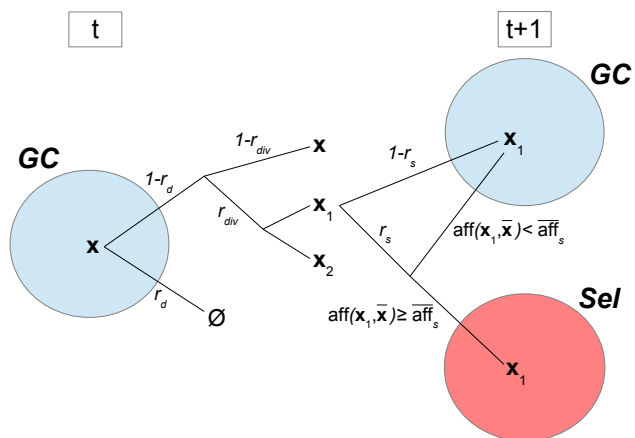
489 Proceeding as in Section 3.2, we can define and study many different models  
 490 of affinity-dependent selection. Here we propose a model in which we perform  
 491 only positive selection and a model reflecting a Darwinian evolutionary system,  
 492 in which the selection is only negative. For the latter, we will take into account  
 493 only  $N + 2$  types instead of  $N + 3$ : we do not have to consider a selected  
 494 pool. Indeed the selected population remains in the GC. Here below we give  
 495 the definitions of both models. In Section 4.1 we formalize these problems  
 496 mathematically, then in Section 4.2 we show some numerical results.

### 497 4.1 Definitions and results

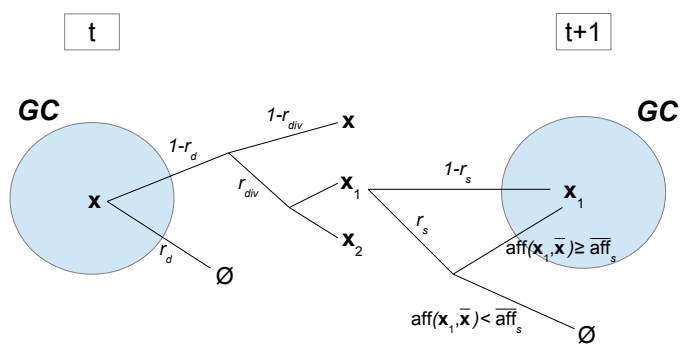
498 Let us consider the process described in Definition 3. We change only the  
 499 selection mechanism.

500 **Definition 10 (Positive selection)** If a B-cell submitted to selection be-  
 501 longs to an affinity class with index greater than  $\bar{a}_s$ , nothing happens. Other-  
 502 wise, the B-cell exits the GC pool and reaches the selected pool.

503 **Definition 11 (Negative selection)** If a B-cell submitted to selection be-  
 504 longs to an affinity class with index greater than  $\bar{a}_s$ , it dies. Otherwise, nothing  
 505 happens.



(a) Positive selection



(b) Negative selection

**Figure 5:** Schematic representations of models described (a) by Definitions 10 and (b) by Definitions 11 of exclusively positive (resp. exclusively negative) selection.

506 In Figure 5 we represent schematically both processes of positive selection  
 507 and of negative selection. It is clear from Figure 5 (b) that in the case of  
 508 Definition 11 we do not need to consider the selected pool anymore.

509 *Positive selection*

510 **Definition 12** Let  $\mathbf{Z}_t^+(\mathbf{i}) = (Z_{t,0}^+(\mathbf{i}), \dots, Z_{t,N+2}^+(\mathbf{i}))$ ,  $t \geq 0$  be a MC where for  
 511 all  $0 \leq j \leq N$ ,  $Z_{t,j}^+(\mathbf{i})$  describes the number of GC B-cells belonging to the  
 512  $j^{\text{th}}$ -affinity class with respect to  $\bar{\mathbf{x}}$ ,  $Z_{t,N+1}^+(\mathbf{i})$  the number of selected B-cells  
 513 and  $Z_{t,N+2}^+(\mathbf{i})$  the number of dead B-cells at generation  $t$ , when the process  
 514 is initiated in state  $\mathbf{i} = (i_0, \dots, i_N, 0, 0)$ , and following the evolutionary model  
 515 described by Definition 10.

516 Let us denote by  $\mathcal{M}^+ = (m_{ij}^+)_{0 \leq i, j \leq N+2}$  the matrix containing the ex-  
 517 pected number of type- $j$  offspring of a type- $i$  cell corresponding to the model  
 518 defined by Definition 10. We can explicitly write the value of all  $m_{ij}^+$  depending  
 519 on  $r_d$ ,  $r_{div}$ ,  $r_s$ , and the elements of matrix  $\mathcal{Q}_N$ .

**Proposition 8**  $\mathcal{M}^+$  is a  $(N+3)^2$  matrix, which we can define as a block matrix in the following way:

$$\mathcal{M}^+ = \begin{pmatrix} \mathcal{M}_1^+ & \mathcal{M}_2^+ \\ \mathbf{0}_{2 \times (N+1)} & \mathcal{I}_2 \end{pmatrix}$$

520 *Where:*

- 521 –  $\mathcal{M}_1^+ = (m_{1,ij}^+)$  is a  $(N+1)^2$  matrix. For all  $i \in \{0, \dots, N\}$ :
- 522 –  $\forall j \leq \bar{a}_s$ :  $m_{1,ij}^+ = 2(1-r_d)r_{div}(1-r_s)q_{ij} + (1-r_d)(1-r_{div})(1-r_s)\delta_{ij}$
- 523 –  $\forall j > \bar{a}_s$ :  $m_{1,ij}^+ = 2(1-r_d)r_{div}q_{ij} + (1-r_d)(1-r_{div})\delta_{ij}$
- 524 where  $\delta_{ij}$  is the Kronecker delta.
- 525 –  $\mathcal{M}_2^+ = (m_{2,ij}^+)$  is a  $(N+1) \times 2$  matrix where for all  $i \in \{0, \dots, N\}$ ,  $m_{2,i1}^+ =$   
 526  $m_{2,i1}$ , and  $m_{2,i2}^+ = r_d$ . We recall that  $m_{2,i1}$  is the  $i^{\text{th}}$ -component of the first  
 527 column of matrix  $\mathcal{M}_2$ , given in Proposition 2.

528 *Negative selection*

529 **Definition 13** Let  $\mathbf{Z}_t^-(\mathbf{i}) = (Z_{t,0}^-(\mathbf{i}), \dots, Z_{t,N+1}^-(\mathbf{i}))$ ,  $t \geq 0$  be a MC where for  
 530 all  $0 \leq j \leq N$ ,  $Z_{t,j}^-(\mathbf{i})$  describes the number of GC B-cells belonging to the  
 531  $j^{\text{th}}$ -affinity class with respect to  $\bar{\mathbf{x}}$  and  $Z_{t,N+1}^-(\mathbf{i})$  the number of dead B-cells  
 532 at generation  $t$ , when the process is initiated in state  $\mathbf{i} = (i_0, \dots, i_N, 0)$ , and  
 533 following the evolutionary model described by Definition 11.

534 Let us denote by  $\mathcal{M}^- = (m_{ij}^-)_{0 \leq i, j \leq N+1}$  the matrix containing the ex-  
 535 pected number of type- $j$  offspring of a type- $i$  cell corresponding to the model  
 536 defined by Definition 13.

**Proposition 9**  $\mathcal{M}^-$  is a  $(N+2)^2$  matrix, which we can define as a block matrix in the following way:

$$\mathcal{M}^- = \begin{pmatrix} \mathcal{M}_1^- & \mathbf{m}_2^- \\ \mathbf{0}'_{N+1} & 1 \end{pmatrix}$$

537 *Where:*

- 538 –  $\mathcal{M}_1^- = (m_{1,ij}^-)$  is a  $(N+1)^2$  matrix. For all  $i \in \{0, \dots, N\}$ :
- 539 –  $\forall j \leq \bar{a}_s$ :  $m_{1,ij}^- = 2(1-r_d)r_{div}q_{ij} + (1-r_d)(1-r_{div})\delta_{ij}$
- 540 –  $\forall j > \bar{a}_s$ :  $m_{1,ij}^- = 2(1-r_d)r_{div}(1-r_s)q_{ij} + (1-r_d)(1-r_{div})(1-r_s)\delta_{ij}$
- 541 –  $\mathbf{m}_2^-$  is a  $(N+1)$  column vector s.t. for all  $i \in \{0, \dots, N\}$   $m_i^+ = m_{2,i2}$ ,
- 542  $m_{2,i2}$  being the  $i^{\text{th}}$ -component of the second column of matrix  $\mathcal{M}_2$ , given
- 543 in Proposition 2.
- 544 –  $\mathbf{0}'_{N+1}$  is a  $(N+1)$  row vector composing of zeros.

545 We do not prove Propositions 8 and 9, since the proofs are the same as for  
546 Proposition 2 (Appendix B).

547

548 Results stated in Proposition 4 hold true for these new models, by simply  
549 replacing matrix  $\mathcal{M}$  with  $\mathcal{M}^+$  (resp.  $\mathcal{M}^-$ ). Of course, in the case of negative  
550 selection, as we do not consider the selected pool, we only refer to (6) and (7)  
551 quantifying the growth and average affinity of the GC. Matrix  $\widetilde{\mathcal{M}}$  is the same  
552 for both models as only selection principles change.

553

554 Because of peculiar structures of matrices  $\mathcal{M}^+$  and  $\mathcal{M}^-$ , we are not able  
555 to compute explicitly their spectra. Henceforth we can not give an explicit  
556 formula for the extinction probability or evaluate the optimal values of the  
557 selection rate  $r_s$  as we did in Sections 3.2 and 3.3.

558

559 Nevertheless, by using standard arguments for positive matrices, the great-  
560 est eigenvalue of both matrices  $\mathcal{M}_1^+$  and  $\mathcal{M}_1^-$  can be bounded, and hence  
561 give sufficient conditions for extinction. Indeed, from classical results about  
562 multi-type GW processes, the value of the greatest eigenvalue allows to dis-  
563 criminate between subcritical case (*i.e.* extinction probability equal to 1) and  
564 supercritical case (*i.e.* extinction probability strictly smaller than 1) [3].

565 **Proposition 10** Let  $\mathbf{q}^+$  (resp.  $\mathbf{q}^-$ ) be the extinction probability of the GC  
566 for the model corresponding to matrix  $\mathcal{M}_1^+$  (resp.  $\mathcal{M}_1^-$ ).

- 567 – If  $r_{div} \leq \frac{r_d}{1-r_d}$ , then  $\mathbf{q}^+ = \mathbf{q}^- = \mathbf{1}$ .
- 568
- 569 – If  $r_s < 1 - \frac{1}{(1-r_d)(1+r_{div})}$ , then  $\mathbf{q}^+ < \mathbf{1}$  and  $\mathbf{q}^- < \mathbf{1}$ .

570 *Proof* Since both matrices  $\mathcal{M}_1^+$  and  $\mathcal{M}_1^-$  are strictly positive matrices, the  
571 Perron Frobenius Theorem insures that the spectral radius is also the greatest  
572 eigenvalue. Then the following classical result holds [23]:

**Theorem 1** Let  $A = (a_{ij})$  be a square nonnegative matrix with spectral radius  $\rho(A)$  and let  $r_i(A)$  denote the sum of the elements along the  $i^{\text{th}}$ -row of  $A$ . Then:

$$\min_i r_i(A) \leq \rho(A) \leq \max_i r_i(A)$$

Simple calculations provide:

$$\begin{aligned}\min_i r_i(\mathcal{M}_1^+) &= (1-r_d)(1+r_{div}) - r_s(1-r_d) \left( 2r_{div} \min_i \sum_{j=0}^{\bar{a}_s} q_{ij} + 1 - r_{div} \right) \\ \max_i r_i(\mathcal{M}_1^+) &= (1-r_d)(1+r_{div}) - 2r_s r_{div} (1-r_d) \max_i \sum_{j=0}^{\bar{a}_s} q_{ij} \\ \min_i r_i(\mathcal{M}_1^-) &= (1-r_d)(1+r_{div}) - r_s(1-r_d) \left( 2r_{div} \min_i \sum_{j=\bar{a}_s+1}^N q_{ij} + 1 - r_{div} \right) \\ \max_i r_i(\mathcal{M}_1^-) &= (1-r_d)(1+r_{div}) - 2r_s r_{div} (1-r_d) \max_i \sum_{j=\bar{a}_s+1}^N q_{ij}\end{aligned}$$

The result follows by observing that for all  $i \in \{0, \dots, N\}$ ,  $0 \leq \sum_{j=0}^{\bar{a}_s} q_{ij}$ ,  $\sum_{j=\bar{a}_s+1}^N q_{ij} \leq 1$ , and applying Theorem 3.  $\square$

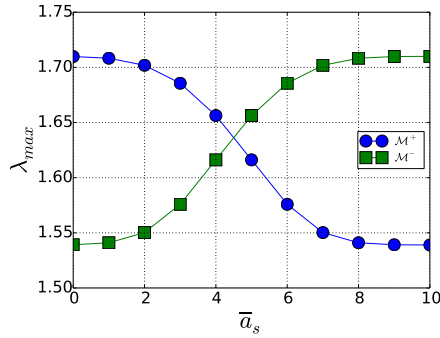


**Figure 6:** Dependence of greatest eigenvalues of matrices  $\mathcal{M}^+$  (blue circles) and  $\mathcal{M}^-$  (green squares) respectively on  $\bar{a}_s$  for  $N = 10$ ,  $r_{div} = 0.9$ ,  $r_d = r_s = 0.1$ . Hence  $(1-r_d)(1+r_{div})(1-r_s) = 1.539$  and  $(1-r_d)(1+r_{div}) = 1.71$ .

573 *Remark 6* One can intuitively obtain the second claim of Proposition 10, as  
 574 this condition over the parameters implies that the probability of extinction  
 575 of the GC for the model underlined by matrix  $\mathcal{M}_1$  of positive and negative  
 576 selection is strictly smaller than 1 (Proposition 1). Indeed keeping the same  
 577 parameters for all models, the size of the GC for the model of positive and  
 578 negative selection is smaller than the size of GCs corresponding to both models  
 579 of only positive and only negative selection. Consequently if the GC corre-  
 580 sponding to  $\mathcal{M}$  has a positive probability of explosion, it will be necessarily  
 581 the same for  $\mathcal{M}^+$  and  $\mathcal{M}^-$ .

582 *Remark 7* The values of both  $\rho(\mathcal{M}_1^+)$  and  $\rho(\mathcal{M}_1^-)$  depend on  $\bar{a}_s$ , varying from  
 583 a minimum of  $(1-r_d)(1+r_{div})(1-r_s)$  and a maximum of  $(1-r_d)(1+r_{div})$ .  
 584 Figure 6 evidences the dependence on  $\bar{a}_s$  of the spectral radius of  $\mathcal{M}_1^+$  and  
 585  $\mathcal{M}_1^-$ , using matrix  $\mathcal{Q}_N$  given by Definition 9 as transition probability matrix.

586 Remark 7 and Figure 6 evidences that, conversely to the previous case  
 587 of positive and negative selection, in both cases of exclusively positive (resp.  
 588 exclusively negative) selection the parameter  $\bar{a}_s$  plays an important role in  
 589 the GC dynamics, affecting its extinction probability. In particular, keeping  
 590 unchanged all other parameters, if  $\bar{a}_s \rightarrow N$  (resp.  $\bar{a}_s \rightarrow 0$ ), then  $\rho(\mathcal{M}_1^+)$  (resp.  
 591  $\rho(\mathcal{M}_1^-)$ )  $\rightarrow (1-r_d)(1+r_{div})(1-r_s)$ , which implies  $\mathbf{q}^+$  (resp.  $\mathbf{q}^-$ )  $\rightarrow \mathbf{1}$ . From  
 592 a biological viewpoint we expect that the GC dynamics should be influenced  
 593 by the threshold required for selection. B-cell affinity determines the ability  
 594 of a B-cell to internalize antigen, and present it to Tfh cells to receive appropriate  
 595 rescue signals. Experimental evidence indicates that B-cell affinity is  
 596 extremely important to determine differential decision in GCs, *i.e.* if a B-cell  
 597 submitted to selection is committed to become either a plasma cell or a mem-  
 598 ory B-cell, recycle back to the dark zone to perform further rounds of somatic  
 599 hypermutations, or die [16].

600

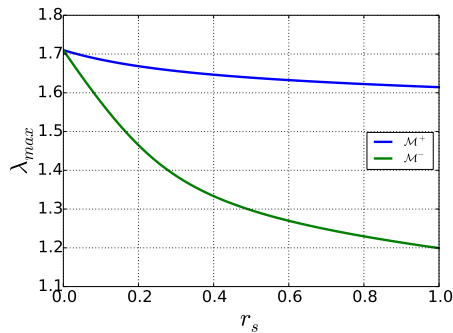


**Figure 7:** Dependence of greatest eigenvalues of matrices  $\mathcal{M}^+$  (blue) and  $\mathcal{M}^-$  (green) respectively on  $r_s$  for  $N = 10$ ,  $r_{div} = 0.9$ ,  $r_d = 0.1$ ,  $\bar{a}_s = 3$ .

601 In Figure 7 we plot the dependence of greatest eigenvalues of both matrices  
 602  $\mathcal{M}^+$  and  $\mathcal{M}^-$  with respect to  $r_s$ . We fix  $r_d = 0.1$  and  $r_{div} = 0.9$  as for Figure  
 603 2. One can note that with this parameter set and if the threshold for positive  
 604 selection  $\bar{a}_s$  is chosen not “too small” nor “too large” with respect to  $N$ , then  
 605 the greatest eigenvalue for both matrices is always greater than 1 independ-  
 606 dently from  $r_s$ , *i.e.* the extinction probability is always strictly smaller than  
 607 1. From a biological viewpoint we expect that a physiological threshold for  
 608 positive selection should not be too strict nor too weak. Indeed, a too demand-  
 609 ing threshold for positive selection is not optimal since B-cells should have

gained an extremely high affinity in order to be positive selected, which would at least require too much time, avoiding a prompt immune response against the invading pathogen. On the other hand, a too weak threshold results in an unchallenging affinity maturation process: almost any B-cell would be positive selected, irrespective from its affinity level with respect to the presented antigen. This could also entail the generation of auto-reactive clones.

## 4.2 Numerical simulations

The evolution of GCs corresponding to matrices  $\mathcal{M}^+$  and  $\mathcal{M}^-$  respectively are complementary. Moreover, in both cases, keeping all parameters fixed one expects a faster expansion if compared to the model of positive and negative selection, since the selection acts only positively (resp. negatively) on good (resp. bad) clones. In particular, the model of negative selection corresponds to the case of 100% of recycling, meaning that all positively selected B-cells stay in the GC for further rounds of mutation, division and selection.

Figure 8 shows the dependence on  $\bar{a}_s$  of the GC size and fitness, comparing  $\mathcal{M}^+$  (left column) and  $\mathcal{M}^-$  (right column). Indeed, for these models the GC dynamics depends on the selection threshold, conversely to the previous case of positive and negative selection, and not only on the selection rate. The effects of  $\bar{a}_s$  on the GC are perfectly symmetric: it is interesting to observe that when both selection mechanisms are coupled, then  $\bar{a}_s$  does not affect the GC dynamics anymore, as shown for instance in Figure 3 (a). Moreover, Figures 8 (c,d) evidence the existence of a value of  $\bar{a}_s$  that minimizes (resp. maximizes) the expected average affinity in the GC for  $\mathcal{M}^+$  (resp.  $\mathcal{M}^-$ ). In both cases this value is approximately  $N/2$ . This certainly depends on the transition probability matrix chosen for the mutational model, which converges to a binomial probability distribution over  $\{0, \dots, N\}$ .

The evolution of the selected pool for the model of positive selection have some important differences if compared to the model described in Section 3. For instance, it is not easy to identify an optimal value of  $r_s$  which maximizes the expected number of selected B-cells at time  $t$ . Indeed it depends both on  $a_0$  and  $\bar{a}_s$ : if  $a_0 \leq \bar{a}_s$  we find curves similar to those plotted in Figure 4 (a), otherwise Figure 9 (a) shows a substantial different behavior. Indeed, if  $a_0 > \bar{a}_s$ , choosing a big value for  $r_s$  does not negatively affect the number of selected B-cells at time  $t$ . In this case, for the first time steps no (or a very few) B-cells will be positively selected, since they still need to improve their affinity to the target. Therefore, they stay in the GC and continue to proliferate for next generations. This fact is further underlined in Figure 9 (b), where we estimate numerically the optimal  $r_s^*$  which maximizes the expected number of selected B-cells at time  $t$ . Simulations show that for  $a_0 \leq \bar{a}_s$  the value of  $r_s^*$  for the model of positive selection is really close to the one obtained by Proposition

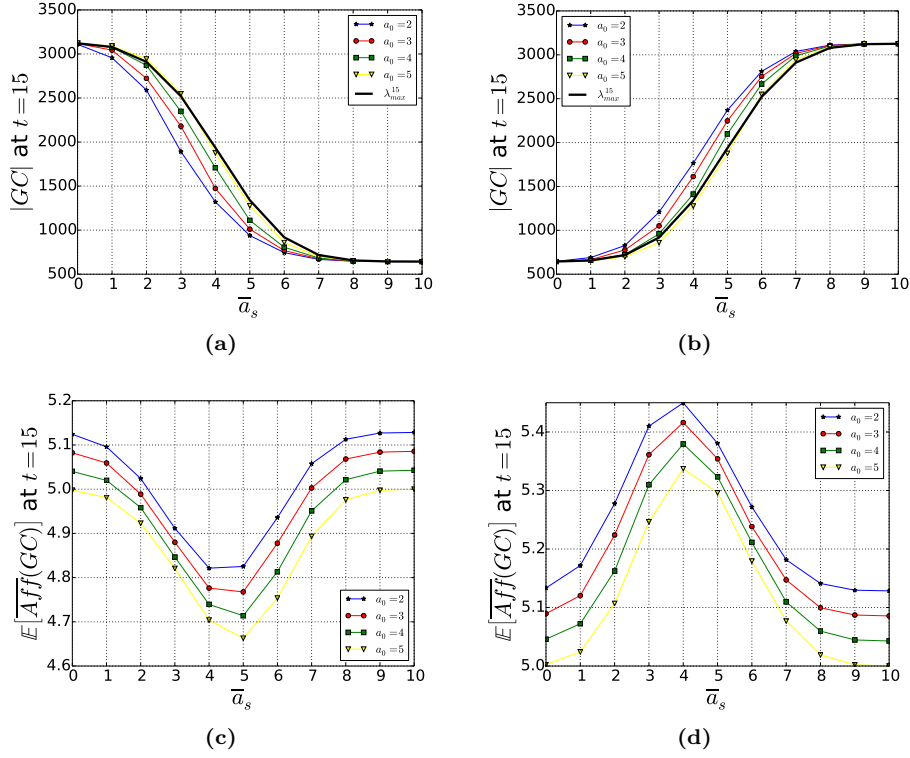


**Figure 8:** (a,b) Dependence of the expected size of the GC after 15 time steps on  $\bar{a}_s$  for different values of  $a_0$ . The thick black line corresponds in both figures to the value of the greatest eigenvalue of matrices  $\mathcal{M}_1^+$  and  $\mathcal{M}_1^-$  respectively, raised to the power of  $t = 15$  (see Figure 6). Note that thanks to Proposition 1 we know that for this parameter choice the expected size of the GC for the model of positive and negative selection corresponds to  $((1 - r_d)(1 + r_{div})(1 - r_s))^{15}$ , which is equivalently  $\lambda_{max}^{15}$  for  $\bar{a}_s = 10$  in Figure 8 (a) or  $\lambda_{max}^{15}$  for  $\bar{a}_s = 0$  in Figure 8 (b). (c,d) Dependence of the expected average affinity in the GC after  $t = 15$  time steps on  $\bar{a}_s$  for different values of  $a_0$ . The left column of Figure 8 refers to the model of positive selection, while the right column to the model of negative selection.

653 **6.** On the other hand if we start from an initial affinity class  $a_0 > \bar{a}_s$  the result  
654 we obtain is substantially different from the previous one, especially for small  
655  $t$ . Moreover we observe important oscillations, which are probably due to the  
656 mutational model, and to the fact that the total GC size is still small for small  
657  $t$ , since the process starts from a single B-cell. Nevertheless, it seems that for  
658  $t$  big enough also in this case the value of  $r_s^*$  tends to approach  $1/t$ .  
659

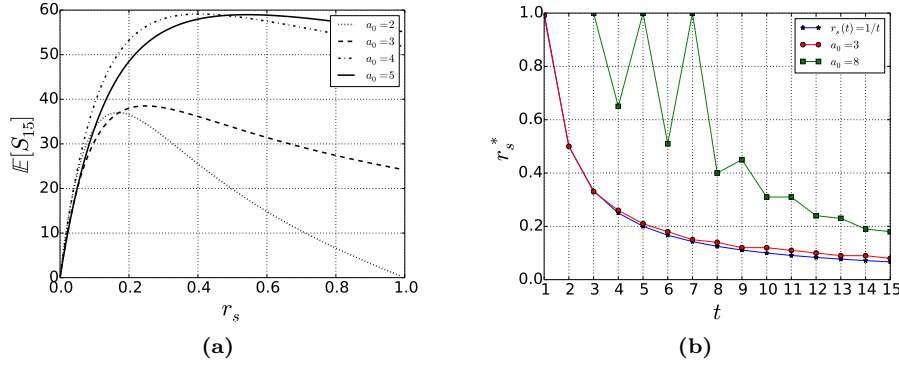


**Figure 9:** Model of positive selection. (a) Expected number of selected B-cells for the time step  $t = 15$  for different values of  $a_0$ , depending on  $r_s$ . (b) Estimation of the optimal  $r_s^*$  maximizing the expected number of selected B-cells for a given generation, comparing the model of positive selection for different values of  $a_0$  and the model described in Section 3 (we plot the exact value,  $r_s(t) = 1/t$ , as obtained by Proposition 6). In (b), for simulations corresponding to the model of positive selection we set  $\bar{a}_s = 5$ .

660 Since in the case of negative selection there is no selected pool, one can  
 661 suppose that at a given time  $t$  the process stops and all clones in the GC pool  
 662 exit the GC as selected clones. Hence it can be interesting to compare the  
 663 selected pool of the model of positive selection and the GC pool of the model  
 664 of negative selection at time  $t$ . Clearly to make these two compartments compar-  
 665 able, the main parameters of both systems have to be opportunely chosen.  
 666 In Figure 10 we compare the size and average fitness of the selected pool for  
 667  $\mathcal{M}^+$  and the GC for  $\mathcal{M}^-$  at time  $t = 30$ . We test different values of the par-  
 668 ameter  $r_s$ . In particular, we observe that increasing  $r_s$  the GC size for the  
 669 model of negative selection decreases and its average fitness increases. For the  
 670 parameter choices we made for these simulations, Figure 10 (a) shows that the  
 671 size of the GC for  $\mathcal{M}^-$  is comparable to the size of the selected pool for  $\mathcal{M}^+$   
 672 at time  $t = 30$  if, keeping all other parameters fixed,  $r_s \in [0.12, 0.15]$ . Never-  
 673 theless, this does not implies a comparable value for the average affinity: the  
 674 clones of the selected pool for  $\mathcal{M}^+$  have a significantly greater average affinity  
 675 than those of the GC for  $\mathcal{M}^-$ . In order to increase the average fitness in the  
 676 GC for the model of negative selection one has to consider greater values for  
 677 the parameter  $r_s$ , but this affects the probability of extinction of the process.  
 678

679 We can expect this discrepancy between the average affinity for the selected  
 680 pool for  $\mathcal{M}^+$  and the one of the GC for  $\mathcal{M}^-$ . Indeed, in the first case we are  
 681 looking to all those B-cells which have been positive selected, hence belong at  
 682 most to the  $\bar{a}_s^{\text{th}}$ -affinity class. On the contrary in the case of  $\mathcal{M}^-$ , we consider  
 683 the average affinity of all B-cells which are still alive in the GC at a given time

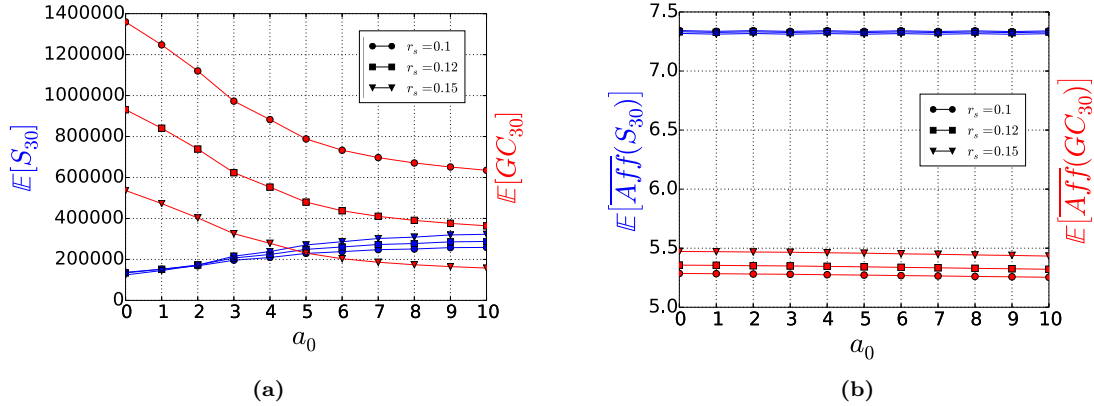


**Figure 10:** Comparison between the pool of selected B-cells for  $\mathcal{M}^+$  (blue) and the GC population for  $\mathcal{M}^-$  (red) at  $t = 30$  for different values of  $r_s$ : (circles)  $r_s = 0.1$ , (squares)  $r_s = 0.12$ , (triangles)  $r_s = 0.15$ . (a) Expected number of B-cells which have been selected until time  $t = 30$  for  $\mathcal{M}^+$  compared to the expected size of the GC for  $\mathcal{M}^-$  at  $t = 30$ . (b) Expected corresponding average affinity for the selected pool (case of positive selection) and the GC (case of negative selection). For some choice of the parameter  $r_s$ , the size of the selected pool for  $\mathcal{M}^+$ , and the GC for  $\mathcal{M}^-$ , are comparable. Nevertheless, the corresponding average affinities are significantly different.

684 step. Among these clones, if  $r_s < 1$ , with positive probability there are also  
 685 individuals with affinity smaller than the one required for escaping negative  
 686 selection. They remain in the GC because they have not been submitted to  
 687 selection. These B-cells make the average affinity decrease. Of course  $r_s$  is not  
 688 the only parameter affecting the quantities plotted in Figure 10. In particular,  
 689 one can observe that choosing a greater value for  $\bar{a}_s$  also have a significant  
 690 effect over the growth of both pools, as discussed in Remark 7.

## 691 5 Conclusions and perspectives

692 In this paper we formalize and analyze a mathematical model describing an  
 693 evolutionary process with affinity-dependent selection. We use a multi-type  
 694 GW process, obtaining a discrete-time probabilistic model, which includes  
 695 division, mutation, death and selection. This is employed in the context of an-  
 696 tibody affinity maturation in GCs. We believe that a probabilistic approach is  
 697 well suited to the study of Darwinian-like processes such as the one taking place  
 698 in GCs during an immune response. Indeed, this kind of approaches allows to  
 699 better take into account local inhomogeneities related to the discrete nature  
 700 of cells and stochastic fluctuations intrinsic to these processes, conversely to

701 more popular deterministic continuum approaches. There, cell concentrations  
702 are described by a set of coupled ODEs changing deterministically and conti-  
703 nuously during time, which has many computational advantages and has often  
704 been employed to model biological systems (*e.g.* [21, 15, 25] for applications to  
705 the GC reaction). In the main model developed here, we choose a selection  
706 mechanism which acts both positively and negatively on individuals submit-  
707 ted to selection. This choice is motivated by the fact that there are biological  
708 evidence supporting both kind of selection mechanisms: positive affinity-based  
709 selection by antigen binding as well as selection-dependent apoptosis [38, 16].  
710 The simplified mathematical framework proposed here allow to investigate how  
711 different kind of B-cell population evolves during the immune response both  
712 in the initial explosion phase and in the later relaxation phase of typical GCs.  
713 Indeed, mathematical analysis of the model leads to build matrix  $\mathcal{M}$ , which  
714 contains the expectations of each type (Proposition 2) and enables to describe  
715 the average behavior of all components of the process. Moreover, thanks to the  
716 spectral decomposition of  $\mathcal{M}$  we were able to obtain explicitly some formulas  
717 giving the expected dynamics of all types. In addition, we exhibited an optimal  
718 value of the selection rate maximizing the expected number of selected clones  
719 for the  $t^{\text{th}}$ -generation (Proposition 6).  
720

721 This is one possible choice of the selection mechanism. From a mathema-  
722 tical point of view, matrix  $\mathcal{M}$  is particularly easy to manipulate, as we can  
723 obtain explicitly its spectrum. On the other hand, the positive and negative  
724 selection model leads, for example, to a selection threshold that does not have  
725 any impact on the evolution of the GC size. From a biological point of view  
726 this seems counterintuitive, since we could expect that the GC dynamics is  
727 sensible to the minimal fitness required for positive selection. Moreover, this  
728 process does not take into account any recycling mechanism, which has been  
729 confirmed by experiments [39] and which improves GCs' efficiency. In addition,  
730 we considered that only the selection mechanism is affinity dependent, while  
731 in the GC reaction other mechanisms, such as the death and proliferation rate,  
732 may depend on fitness [13, 1]. Of course it is possible to define models with  
733 affinity-dependent division and death mechanisms with our formalism. This  
734 would clearly lead to a more complicated model, which can be at least studied  
735 numerically.  
736

737 Mathematical tools used in Section 3 can be applied to define and study  
738 other selection mechanisms. For instance in Section 4 we propose two variants  
739 of the model analyzed in Section 3, in which selection acts only positively, resp.  
740 only negatively. This Section shows how our mathematical environment can  
741 be modified to describe different selection mechanisms, which can be studied  
742 at least numerically. Moreover, it gives a deeper insight of the previous model  
743 of positive and negative selection, by highlighting the effects of each selection  
744 mechanism individually, when they are not coupled.  
745

From a biological viewpoint there exist many possibilities to improve the models proposed in this paper. First of all it is extremely important to fix the system parameters, which have to be consistent with the real biological process. The choice of  $N$  defines the number of affinity level with respect to a given antigen. This value can be interpreted in different ways. On the one hand it can correspond to the number of key mutations observed during the process of Antigen Affinity Maturation, hence be even smaller than 10. On the other hand, each mutational event implies a change in the B-cell affinity, slight or not if it is a key mutation. In this case the affinity can be modeled as a continuous function, hence  $N$  corresponds to a possible discretization [41, 43]. To this choice corresponds an appropriate choice of the transition probability matrix defining the mutational model over the affinity classes,  $\mathcal{Q}_N$ . In most numerical simulations we set  $N = 10$ , which is a sensible value since experimentalists observe that high-affinity B-cells differ in their BCR coding gene by about 9 mutations from germline genes [15, 45]. Nevertheless all mathematical results are independent from this choice and hold true for all  $N \geq 1$ . The selection, division and death rates have also an important impact in the GC and selected pool dynamics: in the simulations we set them in order to be in a case of explosion of the GC hence appreciate the effects of all parameters over the main quantities, but they are not biologically justified. For instance, the typical proliferation rate of a B-cell has been estimated between 2 and 4 per day and in the literature we found B-cell death rates of the order of 0.5-0.8 per day [22, 45, 18]. Hence, if we suppose that a single time step corresponds *e.g.* to 6 hours, a consistent proliferation rate would be  $r_{div} \simeq 0.75$ , while the death rate  $r_d$  should be around 0.175. Since over a 6 hours period about 50% of B-cells transit from the DZ to the LZ, where they compete for positive selection signaling [6, 36], we should choose  $r_s \leq 0.5$ . It could be further characterized taking into account its tightly relation with the time of GC peak, as highlighted in Section 3.3.

In Section 3.3 we have explicitly determined the optimal value of the selection rate maximizing the production of output cells at time  $t$  for the main model of positive and negative selection. It is equal to  $1/t$  independently from all other parameters. Moreover, numerical estimations for the model of positive selection (Section 4.2) suggest that also in this case there exists an optimal value of  $r_s(t)$ , which tends to  $1/t$  at least for  $t$  big enough. One has to interpret this result as the ideal optimal strength of the selection pressure to obtain a peak of the GC production of output cells at a given time step. For example, let us suppose again that a time step corresponds to 6 hours. The peak of the GC reaction has been measured to be close to day 12 [42], *i.e.* after  $\sim 48$  maturation cycles in our model: for the kind of models we built and analyzed in this paper, a constant selection pressure  $r_s$  of  $1/48 \simeq 0.02$  assures that the production of plasma and memory B-cells at the GC peak is maximized. Note that with the parameter choice  $r_d = 0.175$ ,  $r_{div} = 0.75$  and  $r_s = 0.02$ , the extinction probability of the GC is  $\simeq 0.3^{z_0}$ ,  $z_0$  being the number of initial seed cells. Since the extinction probability is strictly smaller than 1, such a GC

will explode with high probability and will be able to assure an intense and efficient immune response.

The particular form  $1/t$  of the optimal selection rate for the  $t^{\text{th}}$  generation obtained in Section 3.3 certainly derives from the simplified structure of the model of positive and negative selection, even if this trend is further confirmed in the model of exclusively positive selection. Nevertheless it should be interesting to test the existence of an inverse relation between the selection rate and the timing of GC peak. Selection pressure can be quantified *e.g.* through comparative analysis between groups of sequences derived from different germline V(D)J segments, as proposed by the statistical framework for Bayesian estimation of Antigen-driven SElectIoN (BASELINE) [44]. BASELINE takes into account both mutation targeting bias and substitution bias and identifies point mutations grouped by location. Moreover it addresses the question of positive versus negative selection: positive selection is identified by an increased frequency of replacements, while a decreased frequency indicates negative selection. According to [44], the selection strength seems to vary and also switch from positive to negative in a different way depending on the location, *i.e.* if we are looking to complementary determining regions (CDRs), which are more significant for functional selection, or to framework regions. This gives stronger motivation to analyse both kind of selection mechanisms, acting both separately and simultaneously, and observe their effects over affinity maturation, as we have done in this paper using our simplified mathematical framework.

In our models the selection pressure is constant. Since the optimal selection rate above depends on time, this suggests to go further in this direction. Moreover, a time-dependent selection pressure would allow to take into account, for instance, the early GC phase in which simple clonal expansion of B-cells with no selection occurs [10]. The hypothesis of a selection pressure changing over time can be easily integrated in our model. Indeed let us suppose that a selection rate  $r_{s,1}$  until time  $t_1$  and  $r_{s,2}$  for all  $t > t_1$  are fixed. Starting from the initial condition  $\mathbf{i}$  the expectations of each type at time  $t$  are given by  $(\mathbf{i}\mathcal{M}_{r_{s,1}}^t)$  if  $t \leq t_1$  and  $(\mathbf{i}\mathcal{M}_{r_{s,1}}^{t_1}\mathcal{M}_{r_{s,2}}^{t-t_1})$  if  $t > t_1$ , where  $\mathcal{M}_{r_{s,i}}$  is the matrix containing the expectations of each type for an evolutionary process with constant selection rate  $r_{s,i}$ ,  $i = 1, 2$ . In Figure 11 we plot the expected evolution during time of all types considering an increasing selection rate. We evaluate the expectations of all types following a process with positive and negative selection. We set  $r_s = 0$  until  $t = 5$ ,  $r_s = 0.1$  from  $t = 6$  to  $t = 15$  and  $r_s = 0.3$  for  $t > 15$ . Numerical simulations show that a time dependent selection rate allows initial explosion of the GC, and then progressive extinction, while when parameters are fixed, a GW process gives only rise either to explosion or to extinction, as shown above. The regulation and termination of the GC reaction has not yet been fully understood. In the literature, an increasing differentiation rate of GC B-cells is thought to be a good explanation [25], here we show that other

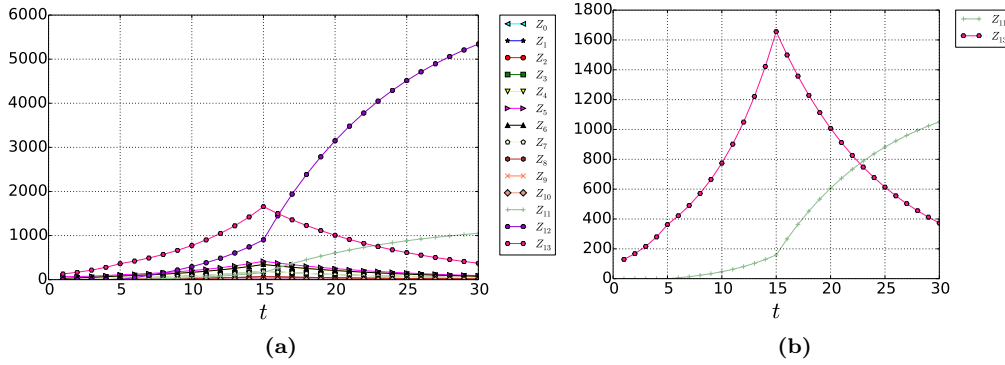


**Figure 11:** (a) Evolution during time of the expected value of all types for the model of positive and negative selection, with  $r_s$  varying during time and  $N = 10$ . In particular we set  $r_s = 0$  until  $t = 5$ ,  $r_s = 0.1$  from  $t = 6$  to  $t = 15$  and  $r_s = 0.3$  from  $t = 16$  to  $t = 30$ .  $Z_{13}$  denotes the total size of the GC (*i.e.*  $\sum_{k=0}^N Z_k$ ), and we recall that  $Z_{11}$  corresponds to selected B-cells and  $Z_{12}$  to dead B-cells. We set  $r_{div} = 0.3$ ,  $r_d = 0.005$  and  $z_0 = 100$  initial naive B-cells. All initial B-cells belong to  $a_0 = 5$ , and the selection threshold is  $\bar{a}_s = 3$ . (b) Evolution during time of the expected total size of the GC and the selected pool respectively, for the same set of parameters as in Figure 11 (a).

837 reasons could be of importance as well. Similarly, we can let other parameters  
 838 vary for fixed time intervals, as well as decide to alternatively switch on and off  
 839 the mutational mechanism, as already proposed in [29]. This can be obtained  
 840 by alternatively use the identity matrix in place of  $Q_N$ .

841

842 Applications of the models presented here to real biological problems and  
 843 data should be further investigated. We propose here some contexts for which  
 844 we believe that our kind of modeling approach could be employed to address  
 845 biologically relevant questions.

846 Even if it is still extremely hard to have precise experimental information  
 847 about the evolution of Antibody Affinity Maturation inside GCs, new refined  
 848 techniques start to be available to measure clonal diversity in GCs. As an ex-  
 849 ample, in [34] the authors combine multiphoton microscopy and sequencing  
 850 to understand how different clonal diversification patterns can lead to efficient  
 851 affinity maturation. The models we propose could be used to infer which are  
 852 reasonable mutational transitional probability matrices and selection mecha-  
 853 nisms/pressure to obtain such different scenario and infer if the tendency of  
 854 GC to go or not through homogenizing selection is solely due to the hazard  
 855 or if this is dependent on the kind of antigenic challenge and/or some specific  
 856 characteristics of the host. If this is the case, these results could be particularly  
 857 relevant *e.g.* in the context of vaccination design, where we are interested in  
 858 find new way to improve the quality of the immune response after vaccination

challenge.

Another potential interesting application field is the study of some diseases entailing a dysfunction of the immune system, such as in particular Chronic Lymphocytic Leukemia (CLL), derived from antigen-experienced B-cells that differ in the level of mutations in their receptors [8]. This is the commonest form of leukemia in the Western world [12]. In CLL, leukemia B-cells can mature partially but not completely, are unable to opportunely undergo mutations in GCs, and survive longer than normal cells, crowding out healthy B-cells. Prognosis varies depending on the ability of host B-cells to mutate their antibody gene variable region. Even if major progresses have been made in the identification of molecular and cellular markers predicting the expansion of this disease in patients, the pathology remains incurable [11,12]. Our modeling approach could be employed to understand how an “healthy” mutational matrix is modified in patients affected by CLL, and if other mechanisms could contribute to get the prognosis worse. This could eventually provide suggestions about the causes that lead to CLL, and motivation for further research on possible treatments.

## 6 Acknowledgements

This work was supported by the Labex inflamex, ANR project 10-LABX-0017.

## References

1. Anderson, S.M., Khalil, A., Uduman, M., Hershberg, U., Louzoun, Y., Haberman, A.M., Kleinstein, S.H., Shlomchik, M.J.: Taking advantage: high-affinity B cells in the germinal center have lower death rates, but similar rates of division, compared to low-affinity cells. *The Journal of Immunology* **183**(11), 7314–7325 (2009)
2. Ansari, H.R., Raghava, G.P.: Identification of conformational B-cell epitopes in an antigen from its primary sequence. *Immunome research* **6**(1), 1 (2010)
3. Athreya, K.B., Ney, P.E.: *Branching processes*, vol. 196. Springer Science & Business Media (2012)
4. Balelli, I., Milisic, V., Wainrib, G.: Branching random walks on binary strings for evolutionary processes in adaptive immunity. arXiv preprint arXiv:1607.00927 (2016)
5. Balelli, I., Milišić, V., Wainrib, G.: Random walks on binary strings applied to the somatic hypermutation of B-cells. *Mathematical biosciences* **300**, 168–186 (2018)
6. Bannard, O., Horton, R.M., Allen, C.D., An, J., Nagasawa, T., Cyster, J.G.: Germinal center centroblasts transition to a centrocyte phenotype according to a timed program and depend on the dark zone for effective selection. *Immunity* **39**(5), 912–924 (2013)
7. Castro, L.N.D., Zuben, F.J.V.: Learning and optimization using the clonal selection principle. *Evolutionary Computation, IEEE Transactions on* **6**(3), 239–251 (2002)
8. Chiorazzi, N., Rai, K.R., Ferrarini, M.: Chronic lymphocytic leukemia. *New England Journal of Medicine* **352**(8), 804–815 (2005)
9. Currin, A., Swainston, N., Day, P.J., Kell, D.B.: Synthetic biology for the directed evolution of protein biocatalysts: navigating sequence space intelligently. *Chemical Society Reviews* **44**(5), 1172–1239 (2015)
10. De Silva, N.S., Klein, U.: Dynamics of B cells in germinal centres. *Nature Reviews Immunology* **15**(3), 137–148 (2015)
11. Dighiero, G., Hamblin, T.: Chronic lymphocytic leukaemia. *The Lancet* **371**(9617), 1017–1029 (2008)

- 905 12. Eichhorst, B., Robak, T., Montserrat, E., Ghia, P., Hillmen, P., Hallek, M., Buske, C.:  
906 Chronic lymphocytic leukaemia: Esmo clinical practice guidelines for diagnosis, treat-  
907 ment and follow-up. *Annals of Oncology* **26**(suppl 5), v78–v84 (2015)
- 908 13. Gitlin, A.D., Shulman, Z., Nussenzweig, M.C.: Clonal selection in the germinal centre  
909 by regulated proliferation and hypermutation. *Nature* (2014)
- 910 14. Harris, T.E.: *The theory of branching processes*. Springer-Verlag (1963)
- 911 15. Iber, D., Maini, P.K.: A mathematical model for germinal centre kinetics and affinity  
912 maturation. *Journal of theoretical biology* **219**(2), 153–175 (2002)
- 913 16. Inoue, T., Moran, I., Shinnakasu, R., Phan, T.G., Kurosaki, T.: Generation of memory  
914 B cells and their reactivation. *Immunological reviews* **283**(1), 138–149 (2018)
- 915 17. Kauffman, S.A., Weinberger, E.D.: The NK model of rugged fitness landscapes and  
916 its application to maturation of the immune response. *Journal of theoretical biology*  
917 **141**(2), 211–245 (1989)
- 918 18. Keşmir, C., De Boer, R.J.: A mathematical model on germinal center kinetics and  
919 termination. *The Journal of Immunology* **163**(5), 2463–2469 (1999)
- 920 19. Kringelum, J.V., Lundegaard, C., Lund, O., Nielsen, M.: Reliable B cell epitope pre-  
921 dictions: impacts of method development and improved benchmarking. *PLoS Comput*  
922 *Biol* **8**(12), e1002829 (2012)
- 923 20. MacLennan, I.C., de Vinuesa, C.G., Casamayor-Palleja, M.: B-cell memory and the  
924 persistence of antibody responses. *Philosophical Transactions of the Royal Society of*  
925 *London B: Biological Sciences* **355**(1395), 345–350 (2000)
- 926 21. Meyer-Hermann, M., Mohr, E., Pelletier, N., Zhang, Y., Vitorica, G.D., Toellner, K.M.:  
927 A theory of germinal center B cell selection, division, and exit. *Cell reports* **2**(1), 162–174  
928 (2012)
- 929 22. Meyer-Hermann, M.E., Maini, P.K., Iber, D.: An analysis of B cell selection mechanisms  
930 in germinal centers. *Mathematical Medicine and Biology* **23**(3), 255–277 (2006)
- 931 23. Minc, H.: *Nonnegative matrices*, 1988 (1988)
- 932 24. Mitchell, R., Kelly, D.F., Pollard, A.J., Trück, J.: Polysaccharide-specific B cell responses  
933 to vaccination in humans. *Human vaccines & immunotherapeutics* **10**(6), 1661–1668  
934 (2014)
- 935 25. Moreira, J.S., Faro, J.: Modelling two possible mechanisms for the regulation of the  
936 germinal center dynamics. *The Journal of Immunology* **177**(6), 3705–3710 (2006)
- 937 26. Murphy, K.M., Travers, P., Walport, M., et al.: *Janeway’s immunobiology*, vol. 7. Gar-  
938 land Science New York, NY, USA (2012)
- 939 27. Pang, W., Wang, K., Wang, Y., Ou, G., Li, H., Huang, L.: Clonal selection algorithm for  
940 solving permutation optimisation problems: A case study of travelling salesman prob-  
941 lem. In: *International Conference on Logistics Engineering, Management and Computer*  
942 *Science (LEMCS 2015)*. Atlantis Press (2015)
- 943 28. Perelson, A.S., Oster, G.F.: Theoretical studies of clonal selection: minimal antibody  
944 repertoire size and reliability of self-non-self discrimination. *Journal of theoretical biol-*  
945 *ogy* **81**(4), 645–670 (1979)
- 946 29. Perelson, A.S., Weisbuch, G.: *Immunology for physicists*. *Reviews of modern physics*  
947 **69**(4), 1219–1267 (1997)
- 948 30. Phan, T.G., Paus, D., Chan, T.D., Turner, M.L., Nutt, S.L., Basten, A., Brink, R.: High  
949 affinity germinal center B cells are actively selected into the plasma cell compartment.  
950 *The Journal of experimental medicine* **203**(11), 2419–2424 (2006)
- 951 31. Shannon, M., Mehr, R.: Reconciling repertoire shift with affinity maturation: the role  
952 of deleterious mutations. *The Journal of Immunology* **162**(7), 3950–3956 (1999)
- 953 32. Shen, W.J., Wong, H.S., Xiao, Q.W., Guo, X., Smale, S.: Towards a mathematical  
954 foundation of immunology and amino acid chains. *arXiv preprint arXiv:1205.6031* (2012)
- 955 33. Shlomchik, M., Watts, P., Weigert, M., Litwin, S.: Clone: a Monte-Carlo computer  
956 simulation of B cell clonal expansion, somatic mutation, and antigen-driven selection.  
957 In: *Somatic Diversification of Immune Responses*, pp. 173–197. Springer (1998)
- 958 34. Tas, J.M., Mesin, L., Pasqual, G., Targ, S., Jacobsen, J.T., Mano, Y.M., Chen, C.S.,  
959 Weill, J.C., Reynaud, C.A., Browne, E.P., et al.: Visualizing antibody affinity matu-  
960 ration in germinal centers. *Science* **351**(6277), 1048–1054 (2016)
- 961 35. Timmis, J., Hone, A., Stibor, T., Clark, E.: Theoretical advances in artificial immune  
962 systems. *Theoretical Computer Science* **403**(1), 11–32 (2008)

- 963 36. Victora, G.D.: Snapshot: the germinal center reaction. *Cell* **159**(3), 700–700 (2014)
- 964 37. Victora, G.D., Mesin, L.: Clonal and cellular dynamics in germinal centers. *Current*  
965 *opinion in immunology* **28**, 90–96 (2014)
- 966 38. Victora, G.D., Nussenzweig, M.C.: Germinal centers. *Annual review of immunology* **30**,  
967 429–457 (2012)
- 968 39. Victora, G.D., Schwickert, T.A., Fooksman, D.R., Kamphorst, A.O., Meyer-Hermann,  
969 M., Dustin, M.L., Nussenzweig, M.C.: Germinal center dynamics revealed by multi-  
970 photon microscopy with a photoactivatable fluorescent reporter. *Cell* **143**(4), 592–605  
971 (2010)
- 972 40. Wang, P., Shih, C.m., Qi, H., Lan, Y.h.: A stochastic model of the germinal center inte-  
973 grating local antigen competition, individualistic T-B interactions, and B cell receptor  
974 signaling. *The Journal of Immunology* p. 1600411 (2016)
- 975 41. Weiser, A.A., Wittenbrink, N., Zhang, L., Schmelzer, A.I., Valai, A., Or-Guil, M.: Affin-  
976 ity maturation of B cells involves not only a few but a whole spectrum of relevant  
977 mutations. *International immunology* **23**(5), 345–356 (2011)
- 978 42. Wollenberg, I., Agua-Doce, A., Hernández, A., Almeida, C., Oliveira, V.G., Faro, J.,  
979 Graca, L.: Regulation of the germinal center reaction by Foxp3+ follicular regulatory  
980 T cells. *The Journal of Immunology* **187**(9), 4553–4560 (2011)
- 981 43. Xu, H., Schmidt, A.G., O'Donnell, T., Therkelsen, M.D., Kepler, T.B., Moody, M.A.,  
982 Haynes, B.F., Liao, H.X., Harrison, S.C., Shaw, D.E.: Key mutations stabilize antigen-  
983 binding conformation during affinity maturation of a broadly neutralizing influenza  
984 antibody lineage. *Proteins: Structure, Function, and Bioinformatics* **83**(4), 771–780  
985 (2015)
- 986 44. Yaari, G., Uduman, M., Kleinstein, S.H.: Quantifying selection in high-throughput im-  
987 munoglobulin sequencing data sets. *Nucleic acids research* **40**(17), e134–e134 (2012)
- 988 45. Zhang, J., Shakhnovich, E.I.: Optimality of mutation and selection in germinal centers.  
989 *PLoS Comput Biol* **6**(6), e1000800 (2010)

## 990 Appendix

### 991 A Few reminders of classical results on GW processes

992 We recall here some classical results about GW processes we employed to derive Proposition  
993 1 (Section 3.1). For further details the reader can refer to [14].

**Definition 14** Let  $X$  be an integer valued rv,  $p_k := \mathbb{P}(X = k)$  for all  $k \geq 0$ . Its probability generating function (pgf) is given by:

$$F_X(s) = \sum_{k=0}^{+\infty} p_k s^k$$

994  $F_X$  is a convex monotonically increasing function over  $[0, 1]$ , and  $F_X(1) = 1$ . If  $p_0 \neq 0$   
995 and  $p_0 + p_1 < 1$  then  $F$  is a strictly increasing function.

**Definition 15** Given  $F$ , the pgf of a rv  $X$ , the iterates of  $F$  are given by:

$$\begin{aligned} F_0(s) &= s \\ F_1(s) &= F(s) \\ F_t(s) &= F(F_{t-1}(s)) \text{ for } t \geq 2 \end{aligned}$$

### 996 Proposition 11

- 997 (i) If  $\mathbb{E}(X)$  exists (respectively  $\mathbb{V}(X)$ ), then  $\mathbb{E}(X) = F'_X(1)$  (respectively  $\mathbb{V}(X) = F''_X(1) -$   
998  $(\mathbb{E}(X))^2 + \mathbb{E}(X)$ ).
- 999 (ii) If  $X$  and  $Y$  are two integer valued independent rvs, then  $X+Y$  is still an integer valued  
1000 rv and its pgf is given by  $F_{X+Y} = F_X F_Y$ .

**Definition 16** We denote by  $\eta$  the extinction probability of the process  $(Z_t)_{t \in \mathbb{N}}$ :

$$\eta := \lim_{t \rightarrow \infty} F_t(0)$$

**Theorem 2**

- 1001 (i) The pgf of  $Z_t^{(z_0)}$ ,  $t \in \mathbb{N}$ , which represents the population size of the  $t^{\text{th}}$ -generation  
 1002 starting from  $z_0 \geq 1$  seed cells, is  $F_t^{(z_0)} = (F_t)^{z_0}$ ,  $F_t$  being the  $t^{\text{th}}$ -iterate of  $F$  (Equation  
 1003 (2)).  
 1004 (ii) The expected size of the GC at time  $t$  and starting from  $z_0$  B-cells is given by:

$$\mathbb{E}(Z_t^{(z_0)}) = z_0 (\mathbb{E}(Z_t)) = z_0 (\mathbb{E}(Z_1))^t, \quad (13)$$

- 1006 (iii)  $\eta$  is the smallest fixed point of the generating function  $F$ , i.e.  $\eta$  is the smallest  $s$  s.t.  
 1007  $F(s) = s$ .  
 1008 (iv) If  $\mathbb{E}(Z_1) =: m$  is finite, then:  
 1009 – if  $m \leq 1$  then  $F$  has only 1 as fixed point and consequently  $\eta = 1$ ;  
 1010 – if  $m > 1$  then  $F$  has exactly a fixed point on  $[0, 1[$  and then  $\eta < 1$ .  
 (v) Denoted by  $\eta_{z_0}$  the probability of extinction of  $(Z_t^{(z_0)})$ , one has:

$$\eta_{z_0} = \eta^{z_0}$$

1011 where  $\eta$  is given by (iii).

1012 Proposition 1 of Section 3.1 follows by applying Theorem 2 and Equation (1).

## 1013 B Proof of Proposition 2

1014 For all  $j \in \{0, \dots, N+2\}$  the generating function of  $Z_j$  gives the number of offspring of each  
 1015 type that a type  $j$  particle can produce. It is defined as follows:

$$f^{(j)}(s_0, \dots, s_{N+2}) = \sum_{k_0, \dots, k_{N+2} \geq 0} p^{(j)}(k_0, \dots, k_{N+2}) s_0^{k_0} \cdots s_{N+2}^{k_{N+2}}, \quad (14)$$

$$0 \leq s_\alpha \leq 1 \text{ for all } \alpha \in \{0, \dots, N+2\}$$

1016 where  $p^{(j)}(k_0, \dots, k_{N+2})$  is the probability that a type  $j$  cell produces  $k_0$  cells of type 0,  $k_1$   
 1017 of type 1, ...,  $k_{N+2}$  of type  $N+2$  for the next generation.

1018 We denote:

- 1019 –  $\mathbf{p}(\mathbf{k}) = (p^{(0)}(\mathbf{k}), \dots, p^{(N+2)}(\mathbf{k}))$ , for  $\mathbf{k} = (k_0, \dots, k_{N+2}) \in \mathbb{Z}_+^{N+3}$   
 1020 –  $\mathbf{f}(\mathbf{s}) = (f^{(1)}(\mathbf{s}), \dots, f^{(N+1)}(\mathbf{s}))$ , for  $\mathbf{s} = (s_0, \dots, s_{N+2}) \in \mathcal{C}^{N+3} := [0, 1]^{N+3}$

1021 Then the probability generating function of  $\mathbf{Z}_1$  is given by:

$$\mathbf{f}(\mathbf{s}) = \sum_{\mathbf{k} \in \mathbb{Z}_+^{N+3}} \mathbf{p}(\mathbf{k}) \mathbf{s}^{\mathbf{k}}, \quad \mathbf{s} \in \mathcal{C}^{N+3} \quad (15)$$

Again, the generating function of  $\mathbf{Z}_t$ ,  $\mathbf{f}_t(\mathbf{s})$ , is obtained as the  $t^{\text{th}}$ -iterate of  $\mathbf{f}$ , and it holds true that:

$$\mathbf{f}_{t+r}(\mathbf{s}) = \mathbf{f}_t[\mathbf{f}_r(\mathbf{s})], \quad \mathbf{s} \in \mathcal{C}^{N+3}.$$

Let  $m_{ij} := \mathbb{E}[Z_{1,j}^{(i)}]$  the expected number of offspring of type  $j$  of a cell of type  $i$  in one generation. We collect all  $m_{ij}$  in a matrix,  $\mathcal{M} = (m_{ij})_{0 \leq i, j \leq N+2}$ . We have [3]:

$$m_{ij} = \frac{\partial f^{(i)}}{\partial s_j}(\mathbf{1})$$

1022 and:

$$\mathbb{E}[Z_{t,j}^{(i)}] = \frac{\partial f_t^{(i)}}{\partial s_j}(\mathbf{1}) \quad (16)$$

1023 Finally:

$$\mathbb{E}[\mathbf{Z}_t^{(1)}] = \mathbf{i}\mathcal{M}^t \quad (17)$$

1024 One can explicitly derive the elements of matrix  $\mathcal{M}$  for the process described in Defini-  
1025 tion 13.

**Proposition**  $\mathcal{M}$  is a  $(N+3) \times (N+3)$  matrix defined as a block matrix:

$$\mathcal{M} = \begin{pmatrix} \mathcal{M}_1 & \mathcal{M}_2 \\ \mathbf{0}_{2 \times (N+1)} & \mathcal{I}_2 \end{pmatrix}$$

1026 Where:

- 1027 –  $\mathbf{0}_{2 \times (N+1)}$  is a  $2 \times (N+1)$  matrix with all entries 0;
- 1028 –  $\mathcal{I}_n$  is the identity matrix of size  $n$ ;
- 1029 –  $\mathcal{M}_1 = 2(1-r_d)r_{div}(1-r_s)\mathcal{Q}_N + (1-r_d)(1-r_{div})(1-r_s)\mathcal{I}_{N+1}$
- 1030 –  $\mathcal{M}_2 = (m_{2,ij})$  is a  $(N+1) \times 2$  matrix where for all  $i \in \{0, \dots, N\}$ :
- 1031 – if  $i \leq \bar{a}_s$ :

$$1032 \quad m_{2,i1} = (1-r_d)(1-r_{div})r_s + 2(1-r_d)r_{div}r_s \sum_{j=0}^{\bar{a}_s} q_{ij},$$

$$1033 \quad m_{2,i2} = r_d + 2(1-r_d)r_{div}r_s \sum_{j=\bar{a}_s+1}^N q_{ij}$$

- 1034 – if  $i > \bar{a}_s$ :

$$1035 \quad m_{2,i1} = 2(1-r_d)r_{div}r_s \sum_{j=0}^{\bar{a}_s} q_{ij},$$

$$1036 \quad m_{2,i2} = r_d + (1-r_d)(1-r_{div})r_s + 2(1-r_d)r_{div}r_s \sum_{j=\bar{a}_s+1}^N q_{ij}$$

1037 *Proof* One has to compute all  $f^{(i)}(\mathbf{s})$  for  $i = 0, \dots, N+2$ , which depend on  $r_d, r_{div}, r_s,$   
1038  $\bar{a}_s$  and the elements of  $\mathcal{Q}_N$ . First, the elements of the  $(N+2)^{\text{th}}$  and  $(N+3)^{\text{th}}$ -lines are  
1039 obviously determined: all selected (resp. dead) cells remain selected (resp. dead) for next  
1040 generations, as they can not give rise to any other cell type offspring (we do not take into  
1041 account here any type of recycling mechanism). Let  $i \in \{0, \dots, N\}$  be a fixed index: we  
1042 evaluate  $m_{ij}$  for all  $j \in \{0, \dots, N+2\}$ . The first step is to determine the value of  $p^{(i)}(\mathbf{k})$  for  
1043  $\mathbf{k} = (k_0, \dots, k_{N+2}) \in \mathbb{Z}_+^{N+3}$ . There exists only a few cases in which  $p^{(i)}(\mathbf{k}) \neq 0$ , which can  
1044 be explicitly evaluated:

$$1045 \quad - p^{(i)}(0, \dots, 0, 1) = \begin{cases} r_d & \text{if } i \leq \bar{a}_s \\ r_d + (1-r_d)(1-r_{div})r_s & \text{otherwise} \end{cases}$$

$$1046 \quad - p^{(i)}(0, \dots, 0, 1, 0) = \begin{cases} (1-r_d)(1-r_{div})r_s & \text{if } i \leq \bar{a}_s \\ 0 & \text{otherwise} \end{cases}$$

$$1047 \quad - p^{(i)}(0, \dots, 0, \underset{i}{1}, 0, \dots, 0, 0) = (1-r_d)(1-r_{div})(1-r_s)$$

$$1048 \quad - p^{(i)}(0, \dots, 0, 2) = (1-r_d)r_{div}r_s^2 \sum_{j_1=\bar{a}_s+1}^N q_{ij_1} \sum_{j_2=\bar{a}_s+1}^N q_{ij_2}$$

$$1049 \quad - p^{(i)}(0, \dots, 0, 2, 0) = (1-r_d)r_{div}r_s^2 \sum_{j_1=0}^{\bar{a}_s} q_{ij_1} \sum_{j_2=0}^{\bar{a}_s} q_{ij_2}$$

$$\begin{aligned}
1050 \quad & - p^{(i)}(0, \dots, 0, 1, 1) = 2(1-r_d)r_{div}r_s^2 \sum_{j_1=0}^{\bar{a}_s} q_{ij_1} \sum_{j_2=\bar{a}_s+1}^N q_{ij_2} \\
1051 \quad & - \text{For all } j_1 < j_2 \in \{0, \dots, N\}: \\
1052 \quad & - p^{(i)}(0, \dots, 0, \underset{j_1}{2}, 0, \dots, 0, 0) = (1-r_d)r_{div}(1-r_s)^2 q_{ij_1}^2 \\
1053 \quad & - p^{(i)}(0, \dots, 0, \underset{j_1}{1}, 0, \dots, 0, \underset{j_2}{1}, 0, \dots, 0, 0) = 2(1-r_d)r_{div}(1-r_s)^2 q_{ij_1} q_{ij_2} \\
1054 \quad & - p^{(i)}(0, \dots, 0, \underset{j_1}{1}, 0, \dots, 0, 1) = 2(1-r_d)r_{div}r_s(1-r_s)q_{ij_1} \sum_{j_2=\bar{a}_s+1}^N q_{ij_2} \\
1055 \quad & - p^{(i)}(0, \dots, 0, \underset{j_1}{1}, 0, \dots, 0, 1, 0) = 2(1-r_d)r_{div}r_s(1-r_s)q_{ij_1} \sum_{j_2=0}^{\bar{a}_s} q_{ij_2} \\
1056 \quad & - p^{(i)}(\mathbf{k}) = 0 \text{ otherwise}
\end{aligned}$$

1057 We can therefore evaluate  $f^{(i)}(\mathbf{s})$ , with  $\mathbf{s} = (s_0, \dots, s_{N+2}) \in \mathcal{C}^{N+3}$ .

1058

1059

For all  $i \leq \bar{a}_s$ :

$$\begin{aligned}
f^{(i)}(\mathbf{s}) &= r_d s_{N+2} + (1-r_d)(1-r_{div})r_s s_{N+1} + (1-r_d)(1-r_{div})(1-r_s)s_i \\
&+ (1-r_d)r_{div}r_s^2 \left( \sum_{j_1=\bar{a}_s+1}^N q_{ij_1} \sum_{j_2=\bar{a}_s+1}^N q_{ij_2} s_{N+2}^2 \right. \\
&+ \left. \sum_{j_1=0}^{\bar{a}_s} q_{ij_1} \sum_{j_2=0}^{\bar{a}_s} q_{ij_2} s_{N+1}^2 + 2 \sum_{j_1=0}^{\bar{a}_s} q_{ij_1} \sum_{j_2=\bar{a}_s+1}^N q_{ij_2} s_{N+1} s_{N+2} \right) \\
&+ (1-r_d)r_{div}(1-r_s)^2 \left( \sum_{j_1=0}^N q_{ij_1}^2 s_{j_1}^2 + 2 \sum_{j_1=0}^N q_{ij_1} \sum_{j_2 < j_1=0}^N q_{ij_2} s_{j_1} s_{j_2} \right) \\
&+ 2(1-r_d)r_{div}r_s(1-r_s) \sum_{j_1=0}^N q_{ij_1} \left( \sum_{j_2=\bar{a}_s+1}^N q_{ij_2} s_{N+2} + \sum_{j_2=0}^{\bar{a}_s} q_{ij_2} s_{N+1} \right) s_{j_1}
\end{aligned} \tag{18}$$

If  $i > \bar{a}_s$  then  $f^{(i)}(\mathbf{s})$  is the same except for the first line, which becomes:

$$(r_d + (1-r_d)(1-r_{div})r_s) s_{N+2} + (1-r_d)(1-r_{div})(1-r_s)s_i$$

The values of each  $m_{ij}$  are now obtained by evaluating all partial derivatives of  $f^{(i)}(\mathbf{s})$  in  $\mathbf{1}$ , keeping in mind that for all  $i \in \{0, \dots, N\}$ ,  $\sum_{j=0}^N q_{ij} = 1$ .  $\square$

## 1060 C Deriving the extinction probability of the GC from the 1061 multi-type GW process (Section 3.2)

1062 Let us recall some results about the extinction probability for multi-type GW processes [3].

1063 **Definition 17** Let  $q^{(i)}$  be the probability of eventual extinction of the process, when it  
1064 starts from a single type  $i$  cell. As above bold symbols denote vectors *i.e.*  $\mathbf{q} := (q^{(0)}, \dots, q^{(N+2)}) \geq$   
1065  $\mathbf{0}$ .

1066 **Definition 18** We say that  $(\mathbf{Z}_t)$  is singular if each particle has exactly one offspring, which  
 1067 implies that the branching process becomes a simple MC.

1068 **Definition 19** Matrix  $\mathcal{M}$  is said to be strictly positive if it has non-negative entries and  
 1069 there exists a  $t$  s.t.  $(\mathcal{M}^t)_{ij} > 0$  for all  $i, j$ .  $(\mathbf{Z}_t)$  is called positive regular iff  $\mathcal{M}$  is strictly  
 1070 positive.

1071 *Notation 1* Let  $\mathbf{u}, \mathbf{v} \in \mathbb{R}^n$ . We say that  $\mathbf{u} \leq \mathbf{v}$  if  $u_i \leq v_i$  for all  $i \in \{1, \dots, n\}$ . Moreover, we  
 1072 say that  $\mathbf{u} < \mathbf{v}$  if  $\mathbf{u} \leq \mathbf{v}$  and  $\mathbf{u} \neq \mathbf{v}$ .

1073 **Theorem 3** Let  $(\mathbf{Z}_t)$  be non singular and strictly positive. Let  $\rho$  be the maximal eigenvalue  
 1074 of  $\mathcal{M}$ . The following three results hold:

- 1075 1. If  $\rho < 1$  (subcritical case) or  $\rho = 1$  (critical case) then  $\mathbf{q} = \mathbf{1}$ . Otherwise, if  $\rho > 1$  (su-  
 1076 percritical case), then  $\mathbf{q} < \mathbf{1}$ .
- 1077 2.  $\lim_{t \rightarrow \infty} \mathbf{f}_t(\mathbf{s}) = \mathbf{q}$ , for all  $\mathbf{s} \in \mathcal{C}^{N+3}$ .
- 1078 3.  $\mathbf{q}$  is the only solution of  $\mathbf{f}(\mathbf{s}) = \mathbf{s}$  in  $\mathcal{C}^{N+3}$ .

1079 The spectrum of matrix  $\mathcal{M}$  defined in Definition 2 (and recalled in Appendix B) is  
 1080 obtained as follows:

1081 **Proposition 12** Let  $\mathcal{M}$  be defined as a block matrix as in Proposition 2. Let  $\lambda_{\mathcal{M},i}$  be its  
 1082  $i^{\text{th}}$ -eigenvalue. The spectrum of  $\mathcal{M}$  is given by:

- 1083 – For all  $i \in \{0, \dots, N\}$ ,  $\lambda_{\mathcal{M},i} = (1 - r_d)(1 - r_s)(1 + r_{div}(2\lambda_i - 1))$ , where  $\lambda_i$  is the  $i^{\text{th}}$ -  
 1084 eigenvalue of matrix  $\mathcal{Q}_N$ .
- 1085 – whereas  $\lambda_{\mathcal{M},N+1} = 1$  with multiplicity 2.

*Proof* As  $\mathcal{M}$  is a block matrix with the lower left block composed of zeros, then  $\text{Spec}(\mathcal{M}) =$   
 $\text{Spec}(\mathcal{M}_1) \cup \text{Spec}(\mathcal{I}_2)$ . The result follows.  $\square$

1086 Therefore we obtain the same condition as in Proposition 1 for the extinction probability  
 1087 in the GC:

1088 **Proposition 13** Let  $\mathbf{q}$  be the extinction probability for the process  $(\mathbf{Z}_t)$  defined in Defini-  
 1089 tion 13 and restricted to the first  $N + 1$  components (i.e. we refer only to matrix  $\mathcal{M}_1$ , which  
 1090 defines the expectations of GC B-cells). Therefore:

- 1091 – if  $r_s \geq 1 - \frac{1}{(1 - r_d)(1 + r_{div})}$ , then  $\mathbf{q} = \mathbf{1}$
- 1092 – otherwise  $\mathbf{q} < \mathbf{1}$  is the smallest fixed point of  $\mathbf{f}(\mathbf{s})$  in  $\mathcal{C}^{N+3}$ .

*Proof*  $\mathcal{Q}_N$  is a stochastic matrix, therefore its largest eigenvalue is 1. The corresponding  
 eigenvalue of matrix  $\mathcal{M}_1$  is:  $\lambda_{\mathcal{M}_1,1} = (1 - r_d)(1 - r_s)(1 + r_{div})$ . The proposition is proved by  
 observing that  $\lambda_{\mathcal{M}_1,1} \leq 1 \Leftrightarrow r_s \geq 1 - \frac{1}{(1 - r_d)(1 + r_{div})}$  and applying Theorem 3 (note that  
 $\mathcal{M}_1$  is positive regular: this is not the case for matrix  $\mathcal{M}$ ).  $\square$

## 1093 D Expected size of the GC derived from the multi-type GW 1094 process (Section 3.2)

**Proposition** Let  $\mathbf{i}$  be the initial state,  $z_0 := |\mathbf{i}|$  its 1-norm ( $|\mathbf{i}| := \sum_{j=0}^{N+2} \mathbf{i}_j$ ). The expected  
 size of the GC at time  $t$ :

$$\sum_{k=0}^N (\mathbf{i}\mathcal{M}^t)_k = |\mathbf{i}| ((1 - r_d)(1 + r_{div})(1 - r_s))^t$$

1095 *Proof* For the sake of simplicity, let us suppose that the process starts from a single B-cell  
 1096 belonging to the affinity class  $a_0 = i$  with respect to the target trait. We do not need to  
 1097 specify the transition probability matrix used to define the mutational model allowed.

1098

We recall the expression of  $\mathcal{M}^t$  obtained by iteration:

$$\mathcal{M}^t = \begin{pmatrix} \mathcal{M}_1^t & \sum_{k=0}^{t-1} \mathcal{M}_1^k \mathcal{M}_2 \\ \mathbf{0}_{2 \times (N+1)} & \mathcal{I}_2 \end{pmatrix}$$

1099 Therefore we can claim that  $(\mathbf{i}\mathcal{M}^t)_k$  corresponds to the  $k^{\text{th}}$ -component of the  $i^{\text{th}}$ -row  
 1100 of matrix  $\mathcal{M}_1^t = (2(1-r_d)r_{div}(1-r_s)\mathcal{Q}_N + (1-r_d)(1-r_{div})(1-r_s)\mathcal{I}_{N+1})^t$ , where  $\mathcal{Q}_N$  is  
 1101 a stochastic matrix. Matrices  $\mathcal{A} := 2(1-r_d)r_{div}(1-r_s)\mathcal{Q}_N$  and  $\mathcal{B} := (1-r_d)(1-r_{div})(1-r_s)\mathcal{I}_{N+1}$   
 1102 clearly commute, therefore:

$$(\mathcal{A} + \mathcal{B})^t = \sum_{j=0}^t C_t^j \mathcal{A}^{t-j} \mathcal{B}^j \quad (19)$$

1103 For all  $j$ ,  $0 \leq j \leq t$ :

$$\begin{aligned} \mathcal{A}^{t-j} \mathcal{B}^j &= 2^{t-j} (1-r_d)^{t-j} r_{div}^{t-j} (1-r_s)^{t-j} (1-r_d)^j (1-r_{div})^j (1-r_s)^j \mathcal{Q}_N^{t-j} \\ &= (1-r_d)^t (1-r_s)^t (2r_{div})^{t-j} (1-r_{div})^j \mathcal{Q}_N^{t-j} \end{aligned}$$

Hence:

$$(\mathcal{A} + \mathcal{B})^t = (1-r_d)^t (1-r_s)^t \sum_{j=0}^t C_t^j (2r_{div})^{t-j} (1-r_{div})^j \mathcal{Q}_N^{t-j}$$

1104 And consequently:

$$\begin{aligned} \sum_{k=0}^N (\mathbf{i}\mathcal{M}^t)_k &= \sum_{k=0}^N (\mathbf{i}(\mathcal{A} + \mathcal{B})^t)_k \\ &= (1-r_d)^t (1-r_s)^t \sum_{j=0}^t C_t^j (2r_{div})^{t-j} (1-r_{div})^j \sum_{k=0}^N (\mathbf{i}\mathcal{Q}_N^{t-j})_k \end{aligned}$$

1105 Since  $\mathcal{Q}_N$  is a stochastic matrix, for all  $n$ ,  $\mathcal{Q}_N^n$  is still a stochastic matrix, *i.e.* the entries of  
 1106 each row of  $\mathcal{Q}_N^n$  sum to 1. Therefore:

$$\begin{aligned} \sum_{k=0}^N (\mathbf{i}\mathcal{M}^t)_k &= (1-r_d)^t (1-r_s)^t \sum_{j=0}^t C_t^j (2r_{div})^{t-j} (1-r_{div})^j \\ &= (1-r_d)^t (1-r_s)^t (2r_{div} + 1 - r_{div})^t = (1-r_d)^t (1-r_s)^t (1+r_{div})^t, \end{aligned}$$

1107 as stated by Equation (3) for  $z_0 = 1$ . This result can be easily generalized to the case of  
 1108  $z_0 \geq 1$  initial B-cells.

## 1109 E Proof of Proposition 5

**Proposition** *Let us suppose that at time  $t = 0$  there is a single B-cell entering the GC belonging to the  $i^{\text{th}}$ -affinity class with respect to the target cell. Moreover, let us suppose that  $\mathcal{Q}_N = R\Lambda_N L$ . For all  $t \geq 1$ , the expected number of selected B-cells at time  $t$ , is:*

$$\mathbb{E}(S_t) = r_s (1-r_s)^{t-1} (1-r_d)^t \sum_{\ell=0}^N (2\lambda_\ell r_{div} + 1 - r_{div})^t \sum_{k=0}^{\bar{a}_s} r_{i\ell} l_{\ell k},$$

1110 *Proof* Let us suppose, for the sake of simplicity, that  $\mathcal{Q}_N$  is diagonalizable:

$$\mathcal{Q}_N = R\Lambda_N L, \quad (20)$$

1111 We can prove by iteration that:

$$\mathcal{M}^t = \begin{pmatrix} \mathcal{M}_1^t & \sum_{k=0}^{t-1} \mathcal{M}_1^k \mathcal{M}_2 \\ \mathbf{0}_{2 \times (N+1)} & \mathcal{I}_2 \end{pmatrix} \quad (21)$$

1112 It follows from (20) and (21) that for all  $t \geq 1$ ,  $\mathcal{M}^t$  can be written as:

$$\mathcal{M}^t = \begin{pmatrix} RD^t L & \left( R \sum_{k=0}^{t-1} D^k L \right) \mathcal{M}_2 \\ \mathbf{0}_{2 \times (N+1)} & \mathcal{I}_2 \end{pmatrix}, \quad (22)$$

1113 where  $D = 2(1-r_d)r_{div}(1-r_s)\Lambda_N + (1-r_d)(1-r_{div})(1-r_s)\mathcal{I}_{N+1}$  is a diagonal matrix. We  
1114 obtain its expression thanks to Proposition 2.

1115

1116 Moreover, by Proposition 3 and Equation (20) we have:

$$\widetilde{\mathcal{M}} = \begin{pmatrix} R\widetilde{D}L & \widetilde{\mathcal{M}}_2 \\ \mathbf{0}_{2 \times (N+1)} & \mathcal{I}_2 \end{pmatrix}, \quad (23)$$

1117 where  $\widetilde{D} = 2(1-r_d)r_{div}\Lambda_N + (1-r_d)(1-r_{div})\mathcal{I}_{N+1}$  is a diagonal matrix.

1118

Proposition 4 claims:

$$\mathbb{E}(S_t) = r_s \sum_{k=0}^{\bar{a}_s} \left( \mathbf{i} \mathcal{M}^{t-1} \widetilde{\mathcal{M}} \right)_k$$

From Equations (22) and (23):

$$\mathcal{M}^{t-1} \widetilde{\mathcal{M}} = \begin{pmatrix} RD^{t-1} \widetilde{D}L & RD^{t-1} L \widetilde{\mathcal{M}}_2 + \left( R \sum_{k=0}^{t-2} D^k L \right) \mathcal{M}_2 \\ \mathbf{0}_{2 \times (N+1)} & \mathcal{I}_2 \end{pmatrix}$$

1119 Since, by hypothesis,  $\mathbf{i} = (0, \dots, 0, 1, 0, \dots, 0, 0)$ , with the only 1 being at position  $i$ ,  $0 \leq i \leq N$ ,

1120 then  $\left( \mathbf{i} \mathcal{M}^{t-1} \widetilde{\mathcal{M}} \right)$  denotes the  $i^{\text{th}}$ -row of matrix  $\mathcal{M}^{t-1} \widetilde{\mathcal{M}}$ . Therefore, we are interested in the

1121 sum between 0 and  $\bar{a}_s$  of the elements of the  $i^{\text{th}}$ -row of matrix  $\mathcal{M}^{t-1} \widetilde{\mathcal{M}}$ , *i.e.* of the  $i^{\text{th}}$ -row  
1122 of matrix  $RD^{t-1} \widetilde{D}L$ , since clearly  $\bar{a}_s \leq N$ .  $D^{t-1} \widetilde{D}$  is a diagonal matrix whose  $\ell^{\text{th}}$ -diagonal  
1123 element is given by:

$$\begin{aligned} \left( D^{t-1} \widetilde{D} \right)_\ell &= (2(1-r_d)r_{div}(1-r_s)\lambda_\ell + (1-r_d)(1-r_{div})(1-r_s))^{t-1} \\ &\quad \cdot (2(1-r_d)r_{div}\lambda_\ell + (1-r_d)(1-r_{div})) \\ &= (1-r_s)^{t-1} (1-r_d)^t (2\lambda_\ell r_{div} + 1 - r_{div})^t \end{aligned}$$

The result follows observing that:  $\left( RD^{t-1} \widetilde{D}L \right)_{ik} = \sum_{\ell=0}^N \left( D^{t-1} \widetilde{D} \right)_\ell r_{i\ell} \ell_k$ .  $\square$

## 1124 F Heuristic proof of Proposition 6

**Proposition** For all  $t \in \mathbb{N}$  the value  $r_s(t)$  which maximizes the expected number of selected B-cells at the  $t^{\text{th}}$  maturation cycle is:

$$r_s(t) = \frac{1}{t}$$

1125 *Hypothesis 1*  $\mathcal{Q}_N$  converges through its stationary distribution, denoted by  $\mathbf{m} = (m_i)$ ,  $i \in$   
1126  $\{0, \dots, N\}$ .

1127 *Hypothesis 2*  $Z_t$  explodes, where  $(Z_t)_{t \in \mathbb{N}}$  is given by Definition 4.

1128 Let  $\tilde{Z}_t$ ,  $t \geq 0$  be the random variable describing the GC-population size at time  $t$  before  
1129 the selection mechanism is performed for this generation. For the sake of simplicity, let us  
1130 suppose  $\tilde{Z}_0 = 1$ .  $(\tilde{Z}_t)_{t \in \mathbb{N}}$  is a MC on  $\{0, 1, 2, \dots\}$ . Denoted by  $\tilde{p}_k := \mathbb{P}(\tilde{Z}_1 = k)$ ,  $k \in \{0, 1, 2\}$ :

$$\begin{cases} \tilde{p}_0 = r_d \\ \tilde{p}_1 = (1 - r_d)(1 - r_{div}) \\ \tilde{p}_2 = (1 - r_d)r_{div} \end{cases} \quad (24)$$

1131 It follows:  $\tilde{m} := \mathbb{E}(\tilde{Z}_1) = (1 - r_d)(1 - r_{div}) + 2(1 - r_d)r_{div} = (1 - r_d)(1 + r_{div})$ .

1132

1133 Conditioning to  $Z_t = k$ ,  $\tilde{Z}_{t+1}$  is distributed as the sum of  $k$  independent copies of  $\tilde{Z}_1$ ,  
1134 which gives:

$$\mathbb{E}(\tilde{Z}_t) = \mathbb{E}(Z_{t-1})\mathbb{E}(\tilde{Z}_1) = \mathbb{E}(Z_1)^{t-1}\mathbb{E}(\tilde{Z}_1) = (1 - r_d)^t(1 + r_{div})^t(1 - r_s)^{t-1} \quad (25)$$

1135 Thanks to Hypotheses 1 and 2, if  $t$  is big enough, there is approximately a proportion  
1136 of  $m_i$  elements in the  $i^{\text{th}}$ -affinity class with respect to  $\bar{\mathbf{x}}$ . Therefore, on average at time  $t$   
1137 there are approximately  $\sum_{i=0}^{\bar{a}_s} m_i \mathbb{E}(\tilde{Z}_t)$  B-cells in the GC belonging to an affinity class with  
1138 index at most equal to  $\bar{a}_s$  with respect to  $\bar{\mathbf{x}}$ , before the selection mechanism is performed  
1139 for this generation. Each one of these cells can be submitted to selection with probability  
1140  $r_s$ , and in this case it will be positively selected. Hence:

$$\mathbb{E}(S_t) \simeq r_s \sum_{i=0}^{\bar{a}_s} m_i \mathbb{E}(\tilde{Z}_t) = (1 - r_d)^t(1 + r_{div})^t(1 - r_s)^{t-1} r_s \sum_{i=0}^{\bar{a}_s} m_i, \quad (26)$$

1141 which is maximized at time  $t \geq 1$  for  $r_s(t) = 1/t$ .

1142 *Remark 8* One observes that the approximation in (26) gives the same value for the optimal  
1143  $r_s(t)$  as in Proposition 6. Nevertheless, it does not allow to describe exactly the behavior of  
1144  $\mathbb{E}(S_t)$ , since it is obtained by approximating the distribution of B-cells in the GC with their  
1145 stationary distribution.